

*Functional studies on Oligotropha
carboxidovorans molybdenum-copper CO
dehydrogenase produced in Escherichia coli*

Paul Kaufmann¹, Benjamin R. Duffus¹, Christian Teutloff² and Silke Leimkühler^{1}*

From the ¹Institute of Biochemistry and Biology, Department of Molecular Enzymology, University of Potsdam, 14476 Potsdam, Germany.

²Institute for Experimental Physics, Free University of Berlin, Arnimallee 14, 14195 Berlin, Germany.

***corresponding author:**

Silke Leimkühler; Department of Molecular Enzymology, Institute of Biochemistry and Biology, University of Potsdam, Karl-Liebknecht-Str. 24-25, 14476 Potsdam, Germany; Tel.: +49-331-977-5603; Fax: +49-331-977-5128; E-mail: sleim@uni-potsdam.de

Running title: Studies on a molybdenum-copper CO dehydrogenase expressed in *E. coli*

The abbreviations used are:

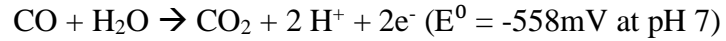
molybdenum cofactor (Moco), molybdopterin (MPT), bis-MPT guanine dinucleotide (bis-MGD), carbon monoxide ehydrogenase (CODH), cytidine-5'-monophosphate (5'CMP), high-performance liquid chromatography (HPLC), electron paramagnetic resonance (EPR), ethylenediaminetetraacetic acid (EDTA), *g*-factor (*g*).

ABSTRACT

The Mo/Cu-dependent CO dehydrogenase (CODH) from *Oligotropha carboxidovorans* is an enzyme that is able to catalyze both the oxidation of CO to CO₂ and the oxidation of H₂ to protons and electrons. Despite the close to atomic resolution structure (1.1 Å), significant uncertainties have remained with regard to the reaction mechanism of substrate oxidation at the unique Mo/Cu-center, as well as the nature of intermediates formed during the catalytic cycle. So far the investigation of the role of amino acids at the active site was hampered due to the lack of a suitable expression system that allowed for detailed site-directed mutagenesis studies at the active-site. Here, we report on the establishment of a functional heterologous expression system of *O. carboxidovorans* CODH in *Escherichia coli*. We characterize the purified enzyme in detail by a combination of kinetic and spectroscopic studies and show that it was purified in a form with comparable characteristics to the native enzyme purified from *O. carboxidovorans*. With this expression system in hand, we were for the first time able to generate active-site variants of this enzyme. Our work presents the basis for more detailed studies on the reaction mechanism for CO and H₂ oxidation of Mo/Cu-dependent CODHs in the future.

INTRODUCTION

Carbon monoxide dehydrogenase (CODH) is a bacterial enzyme that oxidizes CO together with H₂O to yield CO₂, two electrons and two protons (equation 1):



Among the aerobic CODHs the Mo- and Cu-dependent CODH from the α -proteobacterium *Oligotropha carboxidovorans* is one of the most intensely studied enzyme to date. CODH enables the organism to utilize CO as sole energy and carbon source under aerobic chemolithoautotrophic conditions.^{1, 2} The electrons released in the course of the reaction are transferred to the cytoplasmic membrane with quinones functioning as terminal electron acceptors.³ The produced CO₂ is further fixed in the reductive pentose phosphate cycle and is thereby converted to biomass.⁴ CO oxidation is an environmentally crucial reaction since *O. carboxidovorans* contributes to the remediation of approx. 2×10^8 metric tons of atmospheric CO per year.^{5, 6} The enzyme is a molybdenum hydroxylase that is grouped into the xanthine oxidase (XO) family of molybdoenzymes on the basis of its coordination environment at the molybdenum atom.⁷ However, in contrast to the mononuclear molybdenum enzymes, CODH accommodates a unique bimetallic [MoO₂S-Cu] cluster, with the molybdenum atom being embedded to the dithiolene group of the molybdopterin cytosine dinucleotide cofactor (MCD).⁸ The crystal structure revealed that the enzyme is a dimer of two heterotrimers with an overall ($\alpha\beta\gamma$)₂ structure. Each protomer of the enzyme has one small CoxS subunit (17.8 kDa) containing two [Fe₂S₂] clusters, a medium CoxM subunit (30.2 kDa) containing FAD and a large CoxL subunit (88.7 kDa) that binds the bimetallic MCD cofactor. The two metals are bridged by a μ -sulfido ligand while the Cu atom is additionally bound to the Cys388 of the protein backbone, which is located on the VAYRCS³⁸⁸FR active-site loop.^{8, 9} In *O.*

carboxidovorans, the genes encoding for CODH are localized on the megaplasmid pHCG3 in a large *coxBCMSLDEFGHIK* gene cluster comprising twelve genes including the three structural genes *coxMSL*.^{10, 11} The gene products of *coxDEF* were shown to contribute to the posttranslational maturation of the binuclear active-site. The CoxD protein was shown to be an AAA+ ATPase chaperone that is responsible for the insertion of the sulfur ligand, while CoxE and CoxF proteins were proposed to be responsible for insertion of copper into the active-site.¹²⁻¹⁴ CoxF, however, has amino acid sequence homologies to the XdhC protein family shown to be involved in the posttranslational modification and insertion of the sulfido-containing Moco into enzymes of the XO family.¹⁵⁻¹⁷ Since *coxF* mutants contained the MCD cofactor but lacked a sulfido-ligand in addition to Cu with the Mo-site being mainly present as $[\text{Mo}(=\text{O})_2\text{OH}_2]^{14}$, CoxF might be involved in the correct ligation of the Mo-S-Cu group. The CoxG protein is proposed to be a membrane protein attaching CODH to the inner cell membrane.¹²⁻¹⁴ Gene products of *coxBC*, *coxH* and *coxK* were predicted to be membrane localized proteins, with so far unknown function.^{11, 18, 19} The CoxI protein also shares amino acid sequence identities to the XdhC protein^{15-17, 20}, however, its role for CODH maturation has not been characterized to date.

In addition to its CO oxidizing activity, it was reported that the Mo-Cu containing CODH also exhibits hydrogenase activity, oxidizing H₂ to protons.²¹ So far, on the basis of the co-crystal structure with inhibitors in addition to computational studies, several reaction mechanisms have been proposed for CO and H₂ oxidation.^{8, 21-29} At the active site, several amino acids were predicted to play a crucial role in the reaction mechanisms of CO and H₂ oxidation. The highly conserved glutamate residue Glu763, located in close proximity to the equatorial oxygen ligand at the Mo atom, has been proposed to act as active-site base.^{27, 30} By comparison, the Phe390 residue,

located in a flexible loop, has been suggested to play a role in positioning the substrates at the active site. Cys388 was shown to ligate the copper atom. Computational studies suggested that in the course of hydrogen oxidation, protonation of the Cu-coordinated cysteinyl-sulfur is able to trigger the shortening of the Cu-Mo distance, thereby favoring the binding interaction between dihydrogen and copper.²⁵

Due to the lack of a productive heterologous expression system for *O. carboxidovorans* CODH, detailed studies of the reaction mechanism and the exact role of amino acids in the active site were not performed in the past. Heterologous expression of *O. carboxidovorans* CODH in *Escherichia coli* has not been considered for a long time, due to the fact that *E. coli* was thought to be unable to synthesize the MCD cofactor. The discovery of an MCD-containing enzyme in *E. coli* in addition to the identification of the protein which attaches the cytidine-5'-monophosphate (5'-CMP) nucleotide to the molybdopterin-backbone, however, suggested that *E. coli* might indeed be a suitable host for the expression of MCD-containing Mo-Cu containing CODH.^{31, 32}

In this report, a heterologous expression system of *O. carboxidovorans* CODH in *E. coli* was established, which gives rise to active protein. The activity of the wild-type protein after reconstitution with copper and the sulfido ligand was characterized for its activity and spectroscopic properties. CoxI proved to be essential for the insertion of the MCD cofactor into CoxMSL. With this expression system in hand, we were able to generate active-site variants of this enzyme for the first time. Our work presents the basis for more detailed studies to elucidate the role of the amino acids in the reaction mechanism of CO and H₂ oxidation in the future.

MATERIALS AND METHODS

Strains

The bacterial strains and plasmids used in this work are listed in Table 1. Site directed mutagenesis was performed using the Agilent QuikChange Lightning Kit with plasmid pPK2 as template.

Table 1: *E. coli* strains and plasmids used in this study

Strains and plasmids	Description	Source or reference
Plasmid	Genotype	
pTrcHis	Expression vector pTrc _{del} containing the His ₆ -Tag and <i>trc</i> promoter, Amp ^R	³³
pACYC-DuetI	T7-RNA polymerase-based expression vector, Cm ^R	Novagen
pPK1	A 3813-bp PCR fragment containing the coding region of <i>coxMSL</i> cloned into <i>NheI-BamHI</i> of pTrcHis, resulting in a N-terminal His-fusion of CoxM	this work
pPK2	A 7417-bp PCR fragment containing the coding region of <i>coxMSLDEFG</i> cloned into <i>NheI-SacI</i> of pTrcHis, resulting in a N-terminal His-fusion of CoxM	this work
pPK3	A 1198-bp PCR fragment containing the coding region of <i>coxH</i> cloned <i>NdeI-XhoI</i> into MCSI and a 1007-bp PCR fragment containing the coding region for <i>coxI</i> cloned <i>NcoI-HindIII</i> into MCSII of pACYC-DuetI	this work
pPK4	A 1198-bp PCR fragment containing the coding region for <i>coxH</i> cloned <i>NdeI-XhoI</i> into MCSI of pACYC-DuetI	this work
pPK5	A 1007-bp PCR fragment containing the coding region for <i>coxI</i> cloned <i>NcoI-HindIII</i> into MCSII of similarly digested pACYC-DuetI	this work
Strains	Phenotype	
TP1000 (DE3)	F- <i>AlacU169 araD139 rpsL150 relA1 ptsF rbsR flbB ΔmobAB::Kan</i> (DE3)	³⁴
RK5200	F- <i>araD139 ΔlacU169 non rpsL gyrA thi chlA200::Mu cts [moaA]</i>	³⁵

Protein Expression and Purification

Active CODH and variants were expressed after transformation of pPK2 (CoxMSLDEFG) and pPK4 (CoxH and CoxI) into *E. coli* TP1000(DE3) cells.³⁴ The Moco-free apo-CODH was expressed in *E. coli* RK5200(DE3) cells. For expression at 30°C, the main culture was started with an aerobically grown preculture (12h, 37°C

and 220 rpm, supplemented with 150 µg/mL ampicillin and 50 µg/ml chloramphenicol) in a 1:500 dilution. The main culture was supplemented with 150 µg/mL ampicillin, 1 mM molybdate, 20 µM isopropyl β-D-1-thiogalactopyranoside (IPTG) and 100 µM CuCl₂ and proteins were expressed at 30°C and 130 rpm for 24h. For expression at 16°C, the main culture was started with an aerobically grown preculture (12h, 37°C and 220 rpm, supplemented with 150 µg/mL, ampicillin and 50 µg/mL chloramphenicol) in a 1:25 dilution. The main culture was grown in the presence of 150 µg/mL ampicillin and 1 mM molybdate at 37°C and 200 rpm until an OD₆₀₀ of 0.9 was reached. After addition of 20 µM IPTG and 100 µM CuCl₂ the cultures were grown at 16°C and 130 rpm for 24h.

After harvesting of cells and cell lysis, the cleared lysate was applied to 0.5 mL of Ni-nitrilotriacetate (Ni-NTA, Macherey & Nagel, Düren, Germany) resin per liter of cell culture. The resin was washed subsequently with 20 column volumes of 50 mM NaH₂PO₄ buffer, 300 mM NaCl, pH 8.0, containing 10 mM and 20 mM imidazole. Proteins were eluted with 50 mM NaH₂PO₄ buffer, 300 mM NaCl, pH 8.0 containing 250 mM imidazole. Eluted fractions containing CODH were exchanged into 100 mM Tris-HCl, pH 7.2 or in 100 mM potassium phosphate, pH 7.2 buffer using PD-10 columns (GE Healthcare, Piscataway, NJ).

Metal and MCD analysis

Metal analysis was performed using PerkinElmer (Waltham, MA) Life Sciences Optima 2100DV inductively coupled plasma optical emission spectrometer as described earlier.¹⁶ The MCD cofactor was detected fluorometrically after its conversion to FormA-CMP with slight modifications.³⁶ 200 µL of pure protein solution (10 to 20 µM) in 100 mM Tris-HCl, pH 7.2 was oxidized by the addition of

25 μL acidic iodine and incubated over night at room temperature. Excess of iodine was removed by addition of 27.5 μL 1% ascorbic acid and pH was adjusted to 8.3 by addition of 100 μL 1M Tris. Separation of the FormA-CMP fraction was carried out using a C18 reversed phase HPLC column (4.6 * 250 mm ODS Hypersil, Thermo Fisher, particle size 5 μm) equilibrated in 5 mM ammonium acetate and 15% (v/v) methanol. Detection of FormA-CMP during elution was carried out using an Agilent 1100 series fluorescence detector (excitation at 383 nm, emission at 450 nm).

Nucleotide analysis

CMP quantification was performed after the method described by Neumann et al. 2009³¹ with slight modifications. 190 μl of 50-100 μM CO dehydrogenase in 100 mM Tris-HCl, pH7.2 was incubated with 10 μl of concentrated sulfuric acid at 95°C for 30 minutes. Afterwards the samples were centrifuged at 13,000g for 10 minutes. A CMP standard solution in the concentration range of 0 μM to 100 μM was employed for protein derived CMP content calculation. Separation of CMP was carried out using a C18 reversed phase HPLC column (4.6 * 250 mm ODS Hypersil, Thermo Fisher, particle size 5 μm) equilibrated in 50 mM ammonium phosphate, pH 2.5 and 1% (v/v) methanol at an isocratic flow rate of 1 mL/min.

Quantification of the cyanolyzable sulfur

30 to 50 μM of CODH in 100 mM potassium phosphate, pH 7.2 was incubated with 100 mM KCN for 4 to 12 hours at 4°C, using the method described by Massey and Edmondson.³⁷ Released SCN^- was converted to $\text{Fe}(\text{SCN})_2$ and quantified as described previously employing a SCN^- standard solution in the range of 0 to 100 μM .¹⁵

Quantification of FAD

For quantification of FAD, 500 μL of 10 μM CODH in 100 μM Tris-HCl, pH 7.2 were incubated with 60 μL of 50% (w/v) trichloroacetic acid (TCA) for 10 minutes at 4°C. Precipitated protein was pelleted by centrifugation at 15000g for 20 minutes. The protein pellet was washed with 100 μL of 5% (w/v) TCA and centrifuged as described above. The pH of the supernatant was neutralized to 7.0 by the addition of 102 μL of unbuffered 5 M Tris. The FAD content was measured spectroscopically at 450 nm and quantified using a FAD standard curve in the range of 0 to 100 μM .

Enzyme assays

CO oxidation activities were measured as described previously with slight modifications.¹⁰ Anoxic 100 mM potassium phosphate, pH 7.2, containing 123.75 μM INT (2-(4-iodophenyl)-3-(4-nitrophenyl)-5-phenyl tetrazolium chloride), 22.25 μM MPMS (1-Methoxy-5-methylphenazinium methyl sulfate) and 0.5% (w/v) Triton-X100 was bubbled at room temperature in an oxygen-free and rubber sealed flanged rim bottle with pure CO for at least 20 minutes to reach a CO concentration of 1 mM.³⁸ The CO saturated buffer was preheated to 30°C and 1 ml of CO-saturated buffer was transferred with a gas-tight μl -syringe, purged with pure CO, into a N₂-purged septum-sealed cuvette, preheated to 30°C. Activity measurements were started by the addition of 10 μl of 4-40 μM CODH using a gas-tight syringe. CO oxidizing activity was observed spectroscopically by monitoring the reduction of INT at 496 nm. The activity was calculated using the equation $U = (\Delta\text{Abs}_{496}/\text{min})/\epsilon_{496}(\text{INT}) \cdot V$, using the extinction coefficient for INT of 17.98 $\text{mmol}^{-1} \times \text{cm}^{-1}$. One Unit is defined as the oxidation of 1 μmol CO per minute. Variation of CO concentrations for steady state kinetics was achieved by dilution of anoxic,

INT/MPMS-containing CO-saturated buffer with anoxic, INT/MPMS-containing CO-free buffer in serum-stoppered cuvettes directly prior to measurement.

H₂ oxidizing activities were measured as described previously with slight modifications.³⁸ 100 mM potassium phosphate, pH 7.2, containing 50 μM methylene blue was bubbled at room temperature in an oxygen-free and rubber sealed flanged rim bottle with pure molecular hydrogen for at least 100 minutes to reach a H₂ concentration of 780 μM.³⁸ The H₂-saturated buffer was preheated to 30°C and 1 mL of H₂-saturated buffer was transferred with a gas-tight μl-syringe, purged with pure H₂, into a septum sealed cuvette, preheated to 30°C. Measurement was started by the addition of 10 μL of 10-60 μM CODH using a gas-tight Hamilton μL-syringe. H₂ oxidizing activity was recorded spectroscopically by monitoring the reduction of methylene blue at 615 nm. The activity was calculated using the equation $U = (\Delta\text{Abs}_{615}/\text{min})/\epsilon_{615}(\text{methylene blue}) \cdot V$, using the extinction coefficient for methylene blue of 37.11 mmol⁻¹ x cm⁻¹. One Unit is defined as the oxidation of 1 μmol H₂ per minute. Variation of H₂ concentrations for steady state kinetics were achieved by dilution of anoxic, methylene blue-containing H₂-saturated buffer with anoxic, methylene blue-containing H₂-free buffer in serum-stoppered cuvettes directly prior to measurement.

***In vitro* reconstitution of CODH with Sulfide and Copper**

CODH was reconstituted with sulfur and copper as described previously by Resch et al.³⁹ and Wilcoxon et al.³ with slight modifications. All steps of the reconstitution procedure were carried out in an anaerobic chamber (Coy Laboratory Products, Grass Lake, MI) under a mixed Nitrogen/Hydrogen atmosphere (95%/5%). 1 mL of 60 to 70 μM CODH, 10 μl of 10 mM methyl viologen, 10 μL of 10 mM FAD in anoxic

100 mM Tris-HCl, pH 8.2 were mixed before the addition 20 μ L of 100 mM Na₂S and sodium dithionite until the solution reached a light blue color. The sulfuration mixtures were incubated for at least 12 hours in the dark at room temperature or 10°C for CODH variants. After sulfuration, CODH was purified from the incubation mixture by into 100 mM Tris-HCl, pH 7.2 using PD-10 columns under anoxic conditions (GE Healthcare, Piscataway, NJ). Sulfurated CODH was concentrated to a final concentration of 50 to 60 μ M in a volume of 1 ml before the addition of 40 μ L Cu[SC(NH₂)₂]₃Cl in anoxic 100 mM Tris-HCl, pH 7.2. Cu[SC(NH₂)₂]₃Cl was formed by incubation of 10 mM Cu(I)Cl in 100 mM Tris-HCl, pH 7.2 with 10 mM sodium ascorbate and 30 mM thiourea. After incubation for 12 hours at room temperature or at 10 °C over night, small molecular weight compounds were removed by gel filtration using a Superose-12 (GE Healthcare) or a Superdex200 10/300GL column (GE Healthcare) equilibrated in 100 mM Tris-HCl, pH 7.2.

EPR Preparative and Spectroscopic Methods

EPR samples were prepared anaerobically in a Coy chamber at O₂ levels < 10 ppm at 4 °C in a thermoblock, in 100 mM potassium phosphate, pH 7.2. Typical sample preparation methods involved either sample dilution of the concentrated stock enzyme in the above buffer in the as-obtained state (following treatment with KCN or reconstituted as described above), or involved excess addition of freshly-prepared sodium dithionite (11 mM final). Samples were then pipetted into quartz EPR capillaries (3.9 mm O.D.; QSIL, Langewiesen, Germany), sealed and quickly frozen outside of the chamber in liquid N₂-cooled ethanol. Samples containing dithionite were incubated for approximately 20 seconds until freezing.

CW X-Band EPR spectra recorded at 9.4 GHz were obtained using a home-

built spectrometer (microwave bridge, ER041MR, Bruker, Rheinstetten, Germany; lock-in amplifier, SR810, Stanford Research Systems, Stanford, CA, USA; microwave counter, 53181A, Agilent Technologies) equipped with a Bruker SHQ resonator. An ESR 910 helium flow cryostat with an ITC503 temperature controller (Oxford Instruments, Oxfordshire, UK) was used for temperature control. CuEDTA was used as a standard reference with respect to spin quantitation. Spin quantitation was performed using the utility ‘spincounting’ (<http://lcts.github.io/spincounting/>) in Matlab (Mathworks; Natick, MA, USA). Field corrections were performed as needed by measuring a standard solution of sodium dithionite-reduced sample of *R. capsulatus* formate dehydrogenase⁴⁰ (100 μ M) at 80 K under acquisition conditions identical to those reported herein, and correcting with respect to the [Fe₂S₂] clusters present. At this temperature, the [Fe₂S₂] clusters present are nearly identical to those reported for *C. necator* formate dehydrogenase.⁴¹ Measurement parameters for the spectra presented herein were measured with 10 G Modulation Amplitude and 9.9 mW Microwave Power, as reported elsewhere for the natively expressed and reconstituted enzyme²⁶, at a 9.38 GHz Microwave Frequency. Such parameters, while limiting with respect to obtaining resolved ¹H-hyperfine features, have been shown to be sufficient to yield similar spectral features for the natively expressed and reconstituted enzyme.^{26, 42}

RESULTS

Expression and purification of *O. carboxidovorans* CODH after heterologous expression in *E. coli*

For heterologous expression of *O. carboxidovorans* CODH in *E. coli*, the genes *coxMSLDEFG*, *coxH* and *coxI* were amplified from the pHCG3 megaplasmid.¹⁹ We selected a procedure in which we cloned the *coxMSLDEFG* operon into the pTrcHis vector (pPK2), which resulted in a fusion of CoxM with an N-terminal His₆-tag. The genes *coxH* and *coxI* were cloned separately into the pACYC-DuetI vector, allowing the expression of each gene from an own promoter (pPK3). For the expression of CODH, both plasmids were transformed into *E. coli* TP1000(DE3) cells, a strain that proved to be optimal for the expression of molybdoenzymes from the XO family in the past.^{31, 43, 44} Due to a deletion of the *mobAB* genes, the strain is expected to produce higher levels of the molybdopterin cytosine dinucleotide (MCD) cofactor, the variant of Moco present in CODH. The different constructs used for the expression with the combination of different genes are shown in Figure 1.

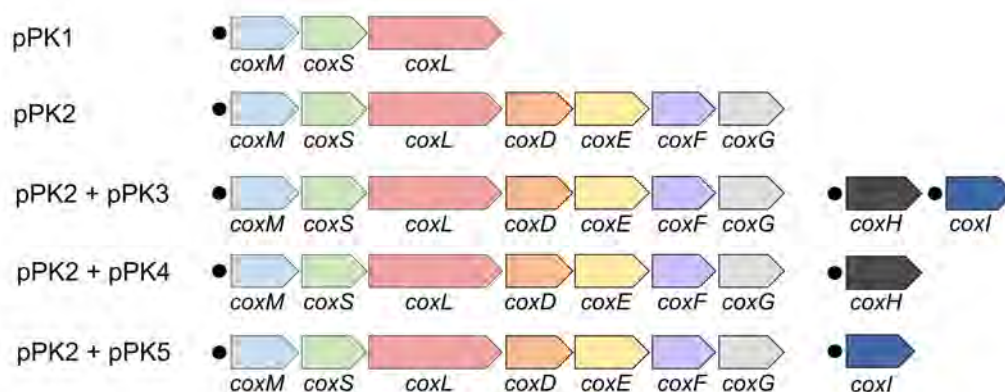


Figure 1: *O. carboxidovorans* CODH genes used for expression in *E. coli*

Shown are the genes encoding CODH and the accessory genes used for the expression in *E. coli* from different plasmids. The plasmid names are shown on the left hand side. Different plasmid combinations were combined to elucidate the minimal requirement for the expression of an active CODH in *E. coli*. Details of the plasmid construction are given in Table 1.

Optimization of the expression conditions showed that both the expression at 30°C and the expression at 16°C gave rise to brownish-colored protein, however, the presence of inclusion bodies was reduced when the temperature during the expression was decreased to 16°C. It has been reported before that CoxD forms inclusion bodies when expressed in *E. coli*.¹² In addition to the temperature, the presence of additional copper was varied during the 16°C expression. The proteins were purified by Ni-NTA and size exclusion chromatography. The elution profile after size exclusion chromatography revealed highly similar elution profiles of the 16°C and 30°C expressed proteins (Figure 2). The majority eluted from the Superdex 200 column in a fraction corresponding to a molecular mass of 285 kDa, which is in good agreement

with the calculated molecular mass of 273 kDa for the $(\alpha\beta\gamma)_2$ hexamer (Figure 2). Minor fractions eluted as $\alpha\beta\gamma$ trimer or $\beta\gamma$ dimer as revealed by SDS-PAGE (Figure 2, inset).

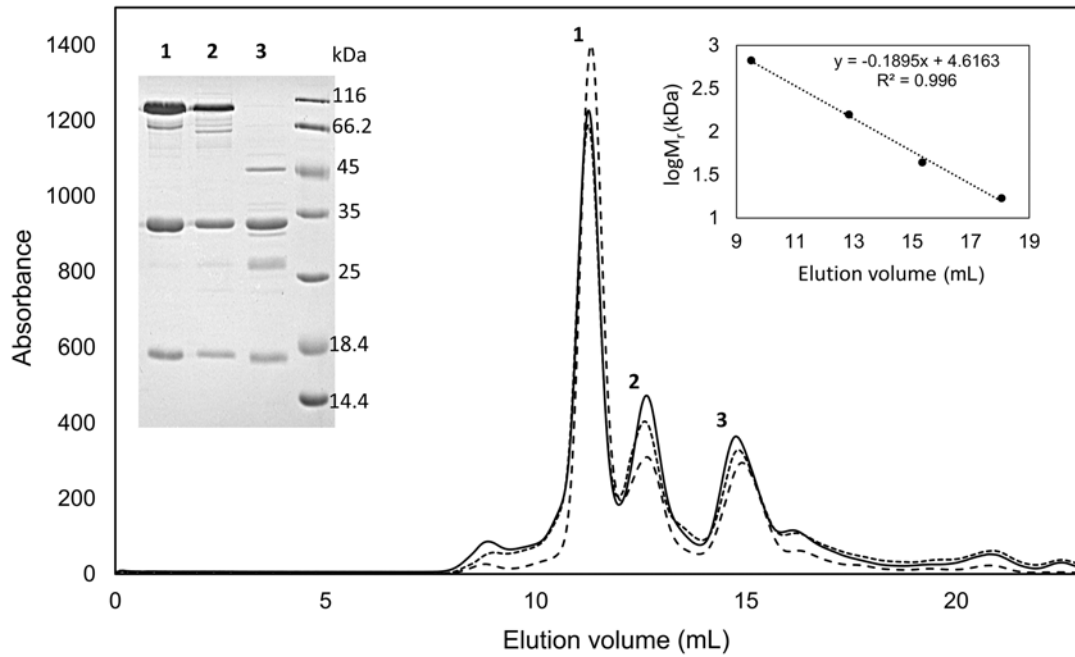


Figure 2: Analysis of the oligomerization state of heterologously expressed CODH by size exclusion chromatography.

100 μ M of purified CODH after expression from plasmids pPK2 (*coxMSLDEFG*) + pPK3 (*coxH* and *coxI*) at 30°C (solid line), at 16°C (dashed line) or from plasmid pPK2 (*coxMSLDEFG*) at 16°C (dotted line) were applied on a Superdex-200 gel-filtration (equilibrated in 100 μ M Tris-HCl, pH 7.2) to determine the oligomerization states. Inset on the left: 17% SDS polyacrylamide gel separating proteins from collected fractions of the elution maxima (marked as 1, 2 and 3) of CODH expressed at 16°C from pPK2 + pPK3. Inset on the right: plot of the standard proteins (Bio-Rad): thyroglobulin (670 kDa), gamma-globulin (158 kDa), ovalbumin (44 kDa), and myoglobin (17 kDa).

The expressed CODH protein at 30°C revealed low CO-oxidizing activities in the as-purified state (below 0.08 U/mg). As reported previously by Resch et al.³⁹, CODH preparations from *O. carboxidovorans* requires an *in vitro* reconstitution of the active-site with copper and sulfur. We therefore applied the same procedure, and after *in*

in vitro reconstitution of the Cu- μ S-ligand to the molybdenum atom, the activity was increased to 0.3 U/mg with CO and 0.038 U/mg with H₂ (Table 2).

Table 2 - Quantification of metals, cofactors and specific activities of CODH expressed in *E. coli* under different conditions.

growth conditions	Yield mg/L culture ^a	Saturation in % ^a					FormA-CMP (LU*s/mg) ^{a,c}	Specific activity in U/mg ^{a,c}	
		Mo ^b	Fe ^b	Cu ^b	FAD ^c	CMP ^c		CO	H ₂
30°C^d +Cu	7	8 ±2	100 ±20	39 ±13	78 ±3	39 ±0.2	388.6	0.3 ±0.01	0.038 ±0.002
16°C^d +Cu	5.9	41 ±7	104 ±8	48 ±7	79 ±7	54 ±10	3550	2.6 ±0.09	0.26 ±0.003
16°C -Cu	6.5	19 ±5.5	104 ±19	15 ±6	93 ±3	43 ±2.5	1613	0.3 ±0.02	0.02 ±0.002

^aSpecific enzyme activities (units/mg) are defined as the oxidation of 1 μ mol substrate/mg enzyme. Molybdenum (μ M molybdenum/ μ M CODH), iron (μ M 2 x [Fe₂S₂]/ μ M CODH) and copper (μ M copper/ μ M CODH) contents were determined by ICP-OES (see Experimental procedures) and related to a fully saturated enzyme. The CMP content (μ M CMP/ μ M CODH) was analyzed after release of CMP from MCD by heat treatment under acidic conditions, as described in Experimental procedures. FormA-CMP was determined after release of MCD from the enzyme under acidic conditions and overnight oxidation with I₂/KI at room temperature. FAD was quantified spectroscopically after TCA precipitation of the protein as described in Experimental procedures.

^bDetermined before *in vitro* reconstitution of the purified enzyme with copper and sulfide.

^cDetermined after *in vitro* reconstitution of the purified enzyme with copper and sulfide.

^dCultures were supplemented with 100 μ M copper during growth.

This value represents about 1.3% of the activity for the CO oxidation reaction reported for the highest active CODH obtained from *O. carboxidovorans* (23.5 U/mg with CO as substrate⁸). The low activity is consistent with a low level of molybdenum present in the enzyme and a low saturation with the MCD cofactor (Table 2). In comparison, the enzyme expressed at 16°C showed a higher molybdenum saturation of 41% and an about 7-fold increased MCD content (Table 2). These values suggest a more efficient MCD cofactor incorporation into recombinant CODH when the

enzyme is expressed at 16°C. However, the iron-, flavin- and copper-contents in both preparations were comparable (Table 2). After reconstitution of the active site with sulfur and copper, the enzyme expressed at 16°C showed a specific activity of 2.6 U/mg, which represents a 9-times higher activity in comparison to the reconstituted enzyme expressed at 30°C. Interestingly, preparation at either temperature resulted in an increased 5'-CMP:Mo saturation ratio (Table 2), suggesting unspecific 5'-CMP binding at the active-site of CODH. The addition of 0.1 mM mM copper during the expression resulted in an almost 10-times more active enzyme, mainly based on the presence of a higher saturation of the enzyme with the MCD cofactor.

The UV-visible spectrum of CODH expressed at 16°C in its oxidized form is similar to the one reported for CODH purified from *O. carboxidovorans* (Figure 3).

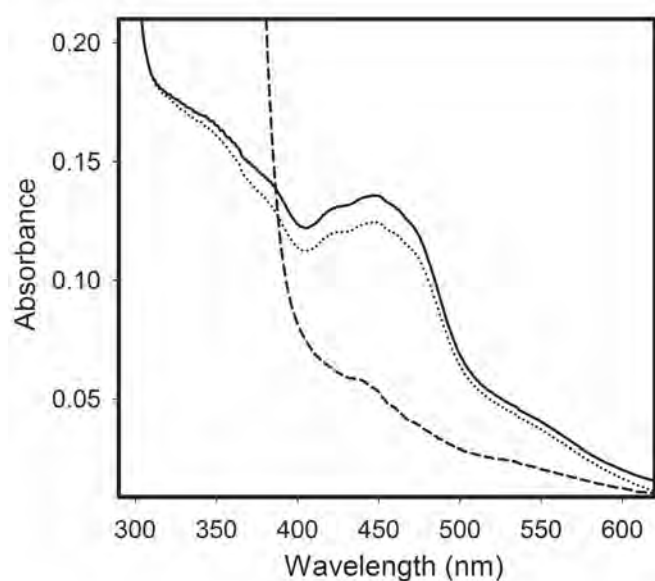


Figure 3: UV-Vis absorption spectra of purified CODH.

UV-visible absorption spectra of purified CODH after expression at 16°C. Shown are the spectra of the oxidized enzyme (solid line) and the spectrum of the enzyme reduced with 950 μM CO (dotted line). Total reduction of the sample was achieved by addition of 10 mM sodium dithionite (dashed line). Spectra were recorded in 100 mM Tris-HCl buffer (pH 7.2). The inset shows the protein separated on a 17% SDS-polyacrylamide gel.

Characteristic are the typical shoulder at 550 nm corresponding to the 2 x [Fe₂S₂] clusters, and the absorption maximum at 450 nm due to the presence of the FAD cofactor. Further, the shoulder at 320 nm represents the sulfido-containing MCD cofactor.⁴⁵ To calculate the amount of catalytically active CODH, reduction spectra were recorded after the addition of 950 μM CO and 10 mM mM sodium dithionite (NDT) (Figure 3). The results show that 13% of the recombinant CODH was reduced with CO, in comparison to the fully reduced enzyme with NDT. The level of reduction is consistent with the determined activity, representing 11% of the fully active CODH from *O. carboxidovorans* (Table 1).

In conclusion for all further analyses, CODH was purified after heterologous expression in *E. coli* choosing a temperature of 16°C and the additional supplementation of copper to the medium.

Steady state kinetics of recombinant CODH

Steady state kinetics of recombinant CODH were carried out under anaerobic conditions at 30°C for the CO:INT/MPMS or H₂:methylene blue reactions. The apparent specific activities for each substrate were plotted against their concentrations and fitted according to the Michaelis-Menten equation. The determined parameters are summarized as insets in Figure 4A and B.

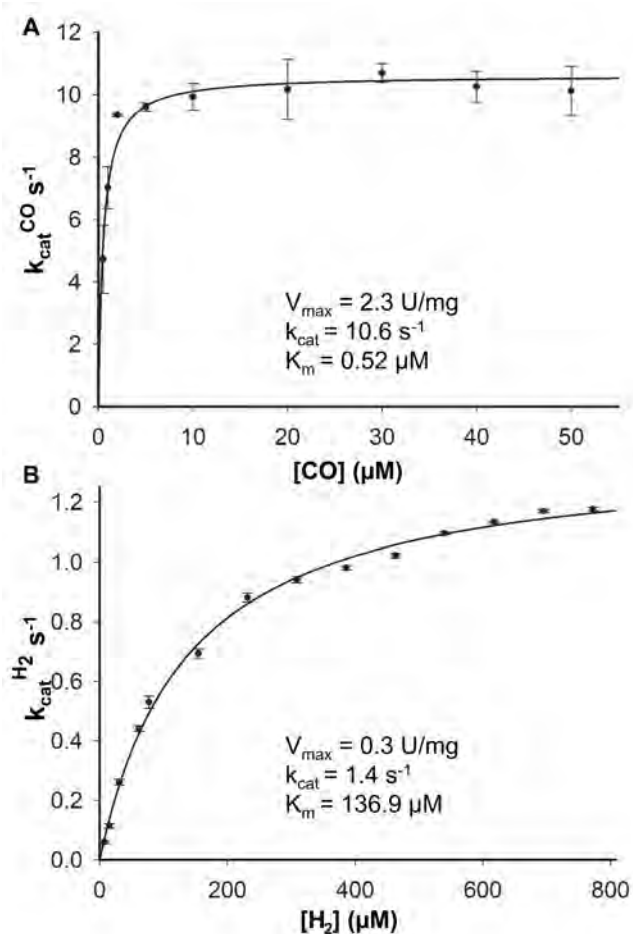


Figure 4: Steady state kinetics of CODH

A, Steady state kinetics of the CO:INT/MPMS reaction. Steady state kinetic parameters of the CO oxidation reaction were recorded at 30°C by monitoring the reduction of INT at 496 nm. CO concentrations were varied from 0-500 μM , while INT/MPMS was used under saturating conditions at a concentration of 123.75 μM and 22.25 μM , respectively. The data were fitted according to the Michaelis Menten equation and are mean values from at least 3 independent measurements. B, Steady state kinetics of the H₂:methylene blue reaction. Steady state parameters were recorded at 30°C by monitoring the reduction of methylene blue at 615 nm. H₂ concentrations were varied from 0-780 μM , while methylene blue used under saturating conditions at a concentration of 50 μM . The data were fitted according to the Michaelis Menten equation and are mean values from at least 3 independent measurements. The determined kinetic constants are depicted as insets.

In consistency with literature data for CODH purified from *O. carboxidovorans*, the hydrogenase activity of recombinant CODH is in the range of 10-16% in relation to the CO oxidizing activity.^{18, 42} The k_{cat} value for CO was determined to be 10.6 s⁻¹

(Figure 4A), showing that the enzyme is 10% active as compared to the fully active enzyme with a k_{cat} value of 107 s^{-1} (with INT/MPMS as electron acceptor) reported by Dobbek et al.⁸. The k_{cat} value for H_2 as substrate was determined as 1.4 s^{-1} (Figure 4B). The K_{M} values were determined as $0.52 \text{ }\mu\text{M}$ for CO and $136.9 \text{ }\mu\text{M}$ for H_2 (Figures 4 A+B).

EPR Spectroscopic Characterization of CODH in *E. coli*

The homogeneity of assembly of the active site for heterologously expressed CODH was assessed by EPR spectroscopy. Figure 5A shows a typical CODH-WT spectrum at 120 K following treatment with KCN in the as-obtained and dithionite-reduced states.

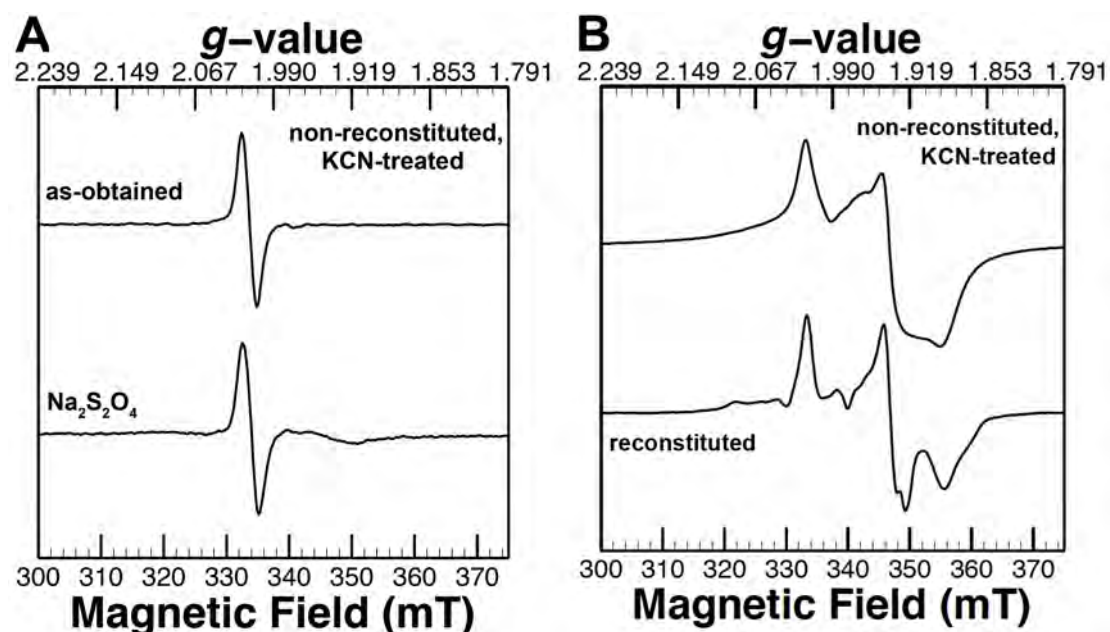


Figure 5: **X-Band EPR spectra of CODH associated Fe-S clusters.** Panel A represents X-band EPR spectra of CODH^{WT} following purification and subsequent treatment with KCN. Shown are spectra of the as-obtained (top trace) and dithionite-reduced (bottom trace) state. Spectra have been dilution factored to have a common [CODH] of $249 \text{ }\mu\text{M}$. Spectra were obtained at 120 K. Panel B represents X-Band EPR spectral comparison of reconstituted and non-reconstituted spectra of $141 \text{ }\mu\text{M}$ CODH^{WT} at 45 K reduced with sodium dithionite. Spectra represent CODH^{WT} as-purified and cyanide-treated (non-reconstituted) (top trace) and CODH^{WT}

reconstituted with Cu(I) thiourea, sulfide, and dithionite (bottom trace). Spectra have been dilution factored to have a common [CODH] noted above. For additional spectral parameters, please see the Materials and Methods section.

The resultant spectra were mostly featureless, aside from an isotropic signal at 333 mT, which is thought to represent a small quantity of FADH• semiquinone.⁴⁶ In the dithionite-reduced state (Figure 5B), at lower temperature a further signal appears, which can be assigned to [Fe₂S₂] clusters, bearing similarity to the type I [Fe₂S₂] cluster reported elsewhere for the natively expressed enzyme.⁴⁷ As can be shown by the decreased linewidth for the [Fe₂S₂] cluster present at 45 K, reconstitution of the active site results in more structurally homogeneous *g*-values for the type I [Fe₂S₂] cluster detected.

Figure 6 depicts a typical CODH-WT sample following reconstitution of the active site sulfane sulfur and Cu. In the as-obtained state, Cu(II) predominates the spectrum (Figure 6A). Signal spin quantitation showed that the as-obtained state displayed 3.1 spins/protein, reflective of excess Cu(II) present in the sample. Interestingly, while Cu(II) appeared to represent the majority of the obtained signal, additional spectral features were observed at 348-360 mT. While these features are small relative to the overall signal, at this field position they are qualitatively similar to the dithionite-reduced CODH from *O. carboxidovorans*.²⁶

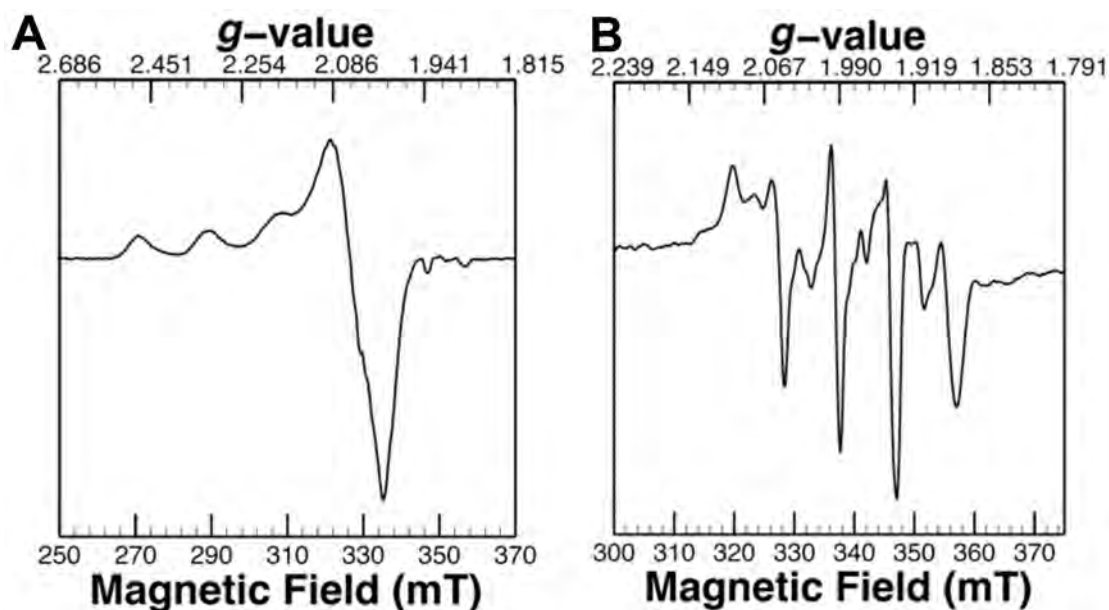


Figure 6: X-Band EPR spectra of CODH after reconstitution with Cu(I) thiourea, sulfide, and dithionite.

Panel A represents the as-obtained enzyme, while panel B represents the sample above following anaerobic reduction with 10 mM dithionite. The spectra have been dilution-factored to represent a [CODH] of 141 μ M. Spectra were obtained at 120 K. For additional spectral parameters, please see the Materials and Methods section.

Treatment of the reconstituted sample with sodium dithionite to CODH-WT resulted in reduction of the excess Cu(II) (Figure 6B), resulting in discernable spectral features similar to that reported for the native *O. carboxidovorans* enzyme.²⁶ The spin concentration decreased from 3.1 spins/protein in the as-obtained (reconstituted) state to 0.5 spins/protein in the dithionite reduced state. Additional components to the spectrum included a decreased, but residual Cu(II) signal, in addition to a small contribution of the FADH• semiquinone radical. No signal corresponding to a desulfo signal was observed. However, since samples were reconstituted in a 3% H₂-containing Coy chamber, it is probable that a small amount of H₂-reduced signal is also present.⁴² Nevertheless, similar reproduction of the dithionite-reduced signal as has been shown for the native *O. carboxidovorans* enzyme demonstrates success in the reconstitution procedure.

Role of the accessory proteins for the maturation of an active CODH in *E. coli*.

In order to define the minimal amount of accessory proteins required for the maturation of *O. carboxidovorans* CODH in *E. coli*, the *coxMSL* genes were expressed in the presence of different genes from the operon and the activity after Ni-NTA affinity purification of the CoxMSL ($\alpha\beta\gamma$)₂ heterotrimer was analyzed. The different coexpression constructs of *coxMSL* with *coxDEFG* and *coxH* or *coxI* are listed in Figure 1.

The expression of the *coxMSL* genes alone (from pPK1) resulted in a colorless and inactive protein that lacked the cofactors and was highly contaminated with other proteins (Figure S1, lane 1). When only the *coxMSLDEFG* operon was expressed (from pPK2) without the coexpression of *coxI* and *coxH*, a CODH with the oligomeric state of a ($\alpha\beta\gamma$)₂ hexamer was obtained (Figure 1 and S1, lane 2). However, the protein was completely inactive and devoid of the MCD cofactor (Figure 7).

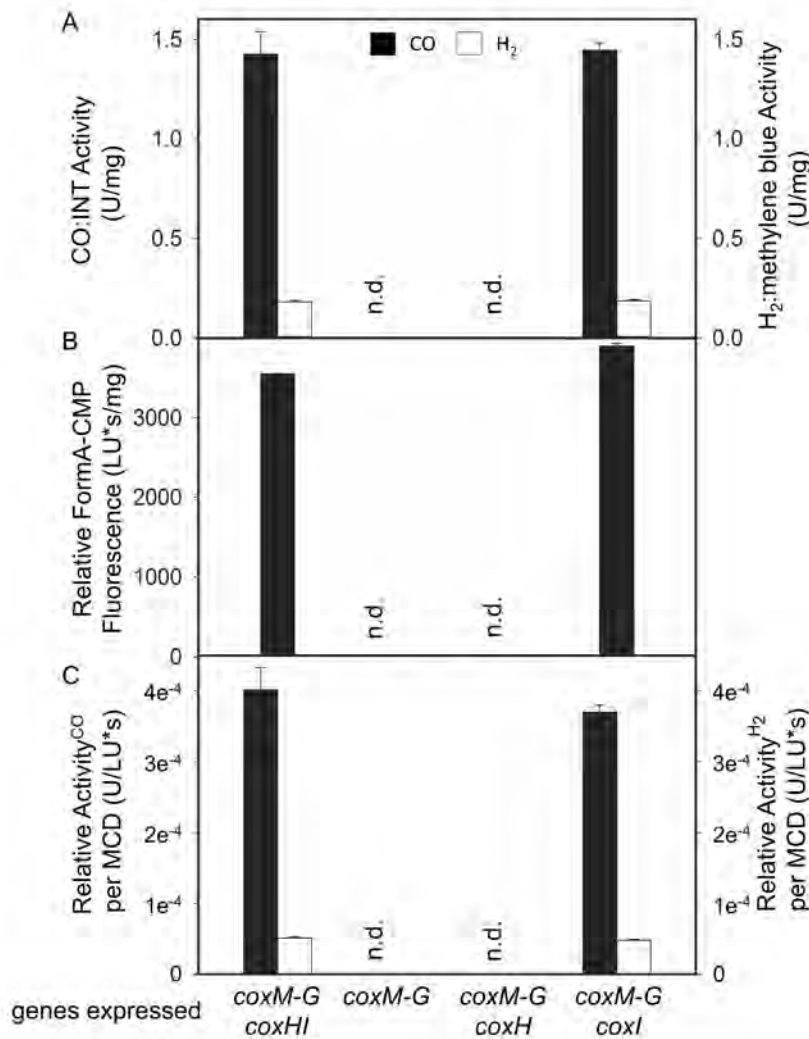


Figure 7: Activities of CO Dehydrogenase expression variants

A, Specific CO or H₂ oxidizing activities (μmol of CO reduced per minute and mg of enzyme) with INT/MPMS or methylene blue as electron acceptors, respectively. Oxidation of substrates was monitored spectroscopically by following the reduction of INT/MPMS (CO) at 496 nm or methylene blue (H₂) at 615 nm. B, Relative FormA-CMP fluorescence (LU*s/mg) of MCD cofactor released from CODH. The MCD cofactor was oxidized to FormA-CMP and quantified after separation on a C18-RP column. Integrated FormA-CMP peak-areas were related to the amount of protein in mg. C, Relative CO or H₂ oxidizing activities in μmol substrate oxidized per MCD present in the protein. n.d.: no activity or FormA-CMP detected

A similar result was obtained when only the *coxH* gene was coexpressed with the *coxMSLDEFG* operon. The protein was purified as a $(\alpha\beta\gamma)_2$ hexamer, but the protein was devoid of the MCD cofactor and consequently completely inactive. In contrast, when the *coxI* gene was coexpressed with the *coxMSLDEFG* operon, an active protein

was obtained with a similar activity as compared to the protein expressed both in the presence of *coxH* and *coxI*. Consequently, *coxH* seems not to be required for the maturation of CoxMSL, while the CoxI protein was essential for the insertion of the MCD cofactor into CoxMSL.

Analysis of the saturation of the proteins with the bound cofactors showed that the proteins were purified with saturation levels of 2 x [Fe₂S₂] clusters and FAD in a range of 80-100% (Table S1). Detection of the saturation levels with molybdenum, the cyanolysable sulfur ligand in addition to CMP revealed unspecific binding of the protein with these metals/molecules, since also a protein that was completely devoid of Moco after expression in a *ΔmoaA* mutant strain showed significant amounts of these atoms/molecules in a range of 10-40%. Especially the presence with copper revealed to be unspecific, since all proteins showed a copper saturation in a range of 43-59%.

Site-directed mutagenesis of amino acid residues at the active site of *O. carboxidovorans* CODH.

The establishment of a heterologous expression system for *O. carboxidovorans* CODH in *E. coli* presented the basis to perform site-directed mutagenesis for analyzing the role of active-site amino acids for CO and H₂ oxidation. In this study, we particularly focused on Glu763, Phe390 and Cys388.

Glu763 is strictly conserved in all members of XO family of molybdoenzymes. Glu763 has been proposed to be involved in proton abstraction during the catalytic cycle of CO oxidation and in addition to facilitate the reversible deprotonation of the copper-bound H₂⁴². We exchanged Glu763 to a glutamine.^{27, 30}

Further, Phe390 was suggested to be involved in substrate binding, and to investigate this role we replaced Phe390 by proline, valine and tyrosine. The phenylalanine is also conserved in other enzymes of the XO family like xanthine dehydrogenase, however, in CODH Phe390 adopts a different conformation to accommodate the additional Cys388 residue that coordinates the copper ion. To test the role of Cys388, we generated a Cys388 deletion variant in CODH.

All variants described above were expressed in *E. coli* and purified by Ni-NTA and size exclusion chromatography after reconstitution of the enzymes with copper and sulfide. The variants were characterized by their absorption spectra before and after the reconstitution with copper and sulfide. As shown in Figure 8, the UV-Vis absorption spectra of all variants in addition to their purities were comparable to the wild-type protein. The yield was the lowest for the F390P variant (supporting Table S2) and all variants showed comparable levels of saturation with 2 x [Fe₂S₂] clusters and FAD.

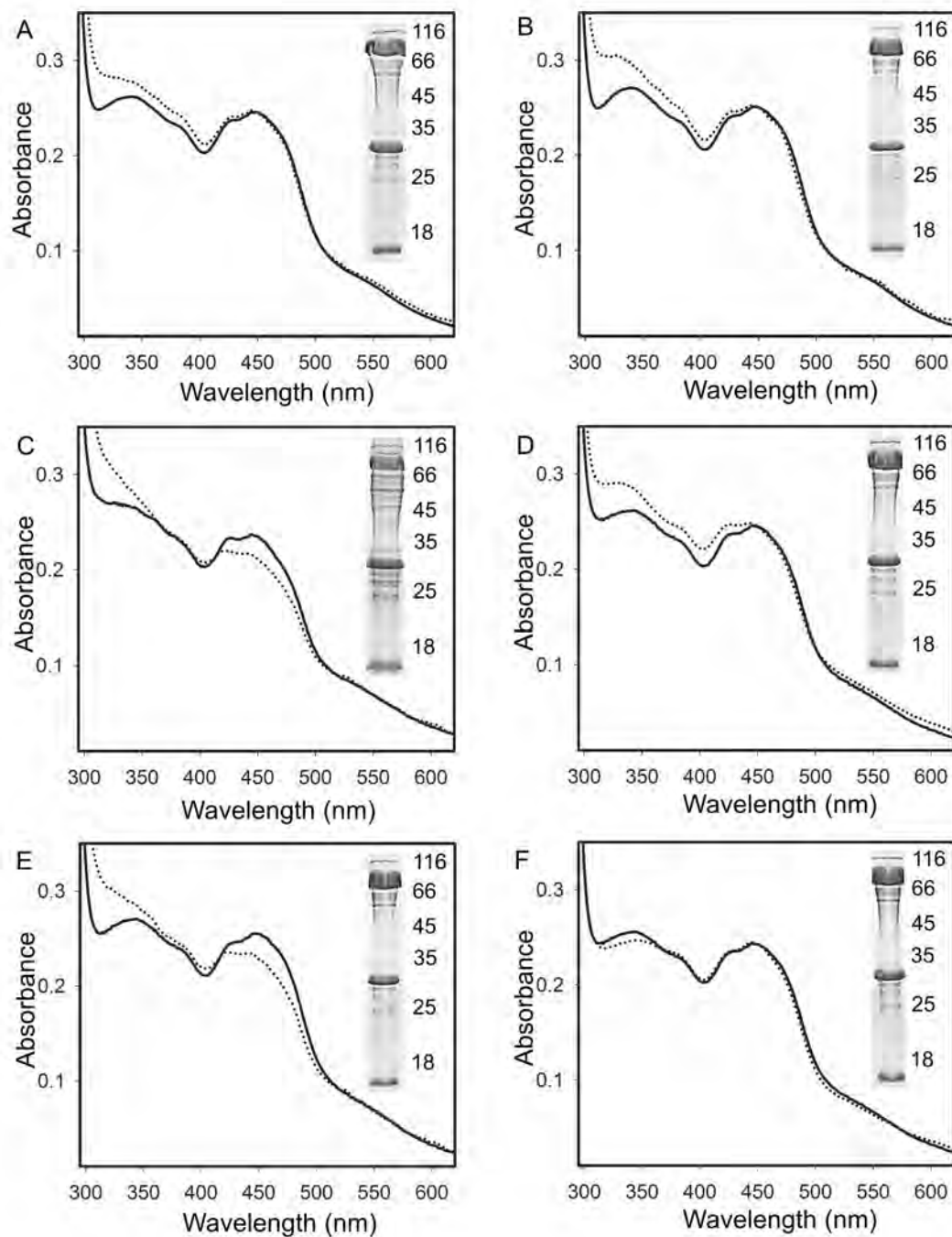


Figure 8: UV-Vis spectra of CODH wild type and variants

UV-Vis spectra of oxidized CODH variants before (solid line) and after (dotted line) reconstitution with sulfide and copper. The spectra were recorded in 100 mM Tris-HCl, pH 7.2. Each insets show a 17% SDS polyacrylamide gel of the indicated CODH variant. A: CODH wild type, B: Variant E763Q, C: Variant F390P, D: Variant F390V, E: Variant F390Y, F: Variant Δ Cys388.

The saturation with molybdenum, copper and CMP varied, however, since it was shown above that these metals/molecules bind unspecific to the protein (Table S2),

we determined the saturation levels with the MCD cofactor instead, assuming that this relates to a specific incorporation. As shown in Figure 9, only the saturation level with MCD of the E763Q variant was comparable to the wild-type protein. In all other variants, the cofactor saturation was largely decreased to levels ranging between 5-10% (F390P and Δ Cys388), 20% (F390V), or 30% (F390Y) in comparison to the MCD content of the wild-type protein. Further, all variants were inactive with CO and H₂ as substrates, with the only exception of the F390Y variant, that revealed specific activities of 40 mU/mg for CO oxidation and 15 mU/mg for H₂ oxidation (Figure 9).

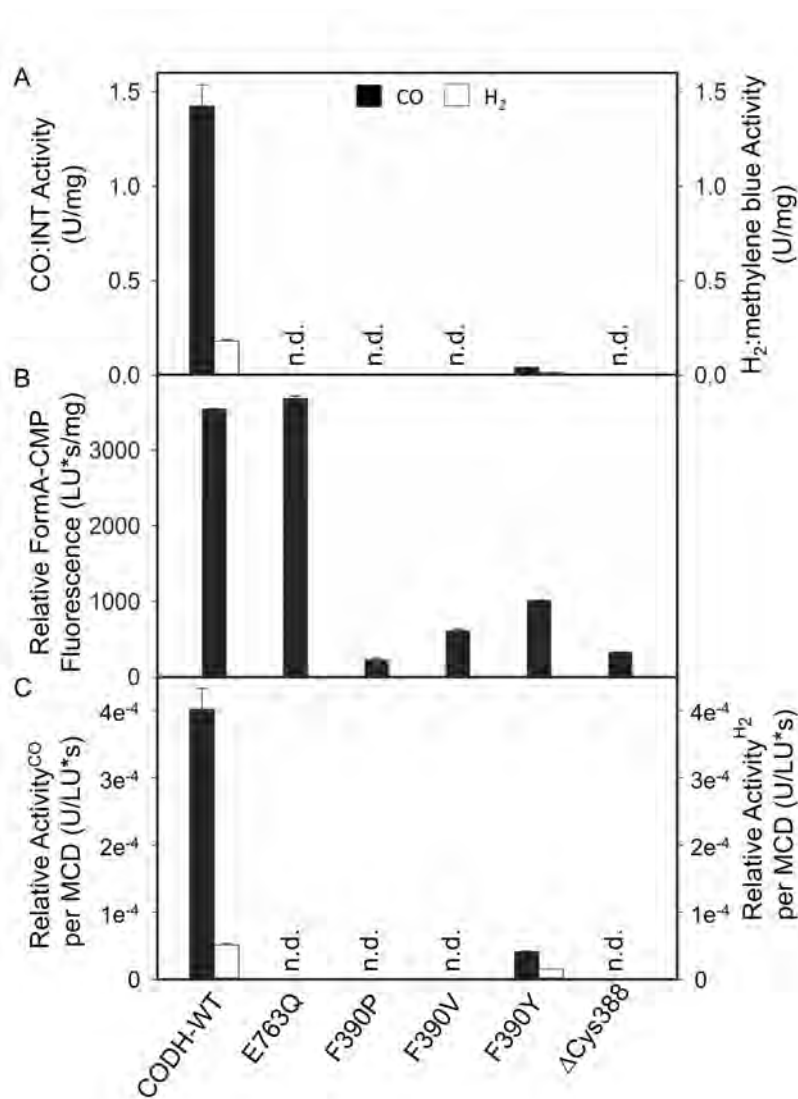


Figure 9: Activities of CO Dehydrogenase active-site variants

A, Specific CO or H₂ oxidizing activities (μmol of CO reduced per minute and mg of enzyme) with INT/MPMS or methylene blue as electron acceptors, respectively. Oxidation of substrates was monitored spectroscopically by following the reduction of INT/MPMS (CO) at 496 nm or methylene blue (H₂) at 615 nm. B, Relative FormA-CMP fluorescence (LU*s/mg) of MCD cofactor released from CODH variants. The MCD cofactor was oxidized to FormA-CMP and quantified after separation on a C18-RP column. Integrated FormA-CMP peak-areas were related to the amount of protein in mg. C, Relative CO or H₂ oxidizing activities in μmol substrate oxidized per MCD present in the protein. n.d.: no activity detected.

The amino acid exchange F390Y thereby had a larger effect on the CO oxidation activity, which was 65 fold reduced, as compared to the H₂ oxidation activity, which was only 17 fold reduced.

To confirm the inactivity of the other variants with both substrates, we additionally performed an in-gel activity staining of the proteins separated on native polyacrylamide gels. This method has the advantage that more protein can be applied and that the electron acceptor precipitates in the gel, so that the activity can be measured over a longer time-range and visualizes also residual activities in a qualitative manner, which would be below the detection limit in the quantitative cuvette assay. As shown in Figure 10 only the F390Y variant showed CO and H₂ oxidizing activities, confirming the activities of the cuvette assays and showing that the E763Q, F390V, F390P and ΔC388 variants were completely inactive.

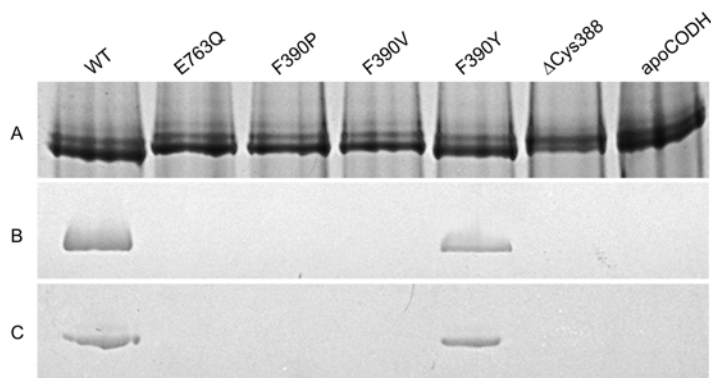


Figure 10: Activity staining of CODH wild type and variants

The figure illustrates 7% native polyacrylamide gels of purified CODH wild type and the indicated variants run under non-denaturing conditions: Gels were stained with (A) Coomassie Brilliant Blue, (B) for CO oxidizing activity or (C) H₂ oxidizing activity after incubation with NBT/PMS. In panel A and B 6 μg of protein were loaded per lane. In panel C 24 μg of protein were lane.

DISCUSSION

In this work we report the first heterologous expression system for the production of active *O. carboxidovorans* CODH in *E. coli*. In previous attempts only the *coxMSL* genes were expressed in *E. coli*, which resulted in an inactive enzyme that was devoid of Moco.²⁶ Our work showed that for the correct MCD insertion into CODH, the gene products CoxDEFG and CoxI are essential. While the role of CoxDEFG in this process has been investigated before, our work presents a novel role of CoxI in MCD insertion into CoxL. We propose that CoxI and CoxDEFG work in conjunction for the insertion and the correct assembly of the MCD-Cu-sulfido cluster into CODH. CoxD was predicted previously to act as an ATP-dependent chaperone that interacts with CoxE and CoxF for the sulfane sulfur insertion into the MoO₃ on the MCD cofactor, with the role of the CoxF and CoxE proteins being proposed to facilitate the insertion of the Cu(I) atom.¹²⁻¹⁴ Since both CoxF and CoxI share amino acid sequence homologies to the XdhC protein, which was proposed to be involved in the maturation of *R. capsulatus* xanthine dehydrogenase by binding the Mo-MPT cofactor for the insertion of the sulfido ligand and further insertion into the XDH enzyme, both CoxF and CoxI might act in a similar and concerted manner. We propose that CoxI might act as a scaffold for MCD binding and by involvement of CoxDEF the Cu-sulfido ligands are assembled. The additional predicted roles of CoxDEF as DEAD box proteins involved in translational processes is not clear in the course of MCD-S-Cu maturation, but might imply a coordinated translation of all three proteins to ensure their presence in equal amounts.

A study by Santiago et al.¹¹ reported on the transposon mutagenesis of *O. carboxidovorans*, to create a knock out of *coxH* and *coxI*. This study showed that in

O. carboxidovorans CoxH and CoxI are not essential for the synthesis of active CODH¹¹. Further, a recent publication by Heinrich et al.⁴⁸ reported the heterologous expression of *O. carboxidovorans* CODH in *Ralstonia eutropha*. This report describes the successful expression of the *coxMSLDEFG* operon without the coexpression of *coxI* that yielded an inactive protein. Since both in *O. carboxidovorans* and *R. eutropha* *coxI* is not essential, we only can speculate that either another protein can take over the role of CoxI in these two organisms, or alternatively, that CoxF is able to replace the role of CoxI in this process, based on the amino acid sequence identities of both protein. CoxF might not be correctly folded in *E. coli*, the reason why the role of CoxI is indispensable in this organism.

Our report also revealed unspecific molybdenum, copper and MCD binding to the heterologously expressed proteins. Unspecific binding of nucleotides was also reported for *Hydrogenophaga pseudoflava* CODH expressed under molybdenum-deficient conditions.^{49, 50} While the protein expressed under molybdenum-free conditions was devoid of the MCD cofactor, the presence of different cytidine nucleotides in the protein was detected.^{49, 50} Thus, unspecific binding of metals and nucleotides might be a common feature also for other molybdoenzymes after overexpression in homologous or heterologous hosts, therefore the activity of the protein should be related to the active portion of the fully matured Moco present in the enzyme, and not solely to the amount of molybdenum or nucleotides present in the protein.

The CODH produced in this work showed an activity of 10% in comparison to the most active CODH reported in the literature.⁸ However, in several reports, also the activity of the CODH purified from its native host varied and often activities are reported ranging about about 18 - 107 s⁻¹.^{9, 12, 14, 22, 46} When comparing our data to

those reported by Wilcoxon et al.⁴², the k_{cat} value for H₂ is 27% of their value for the H₂:1,4-benzoquinone reaction, with the K_M values being comparable. As discussed above the relatively low activity of recombinant CODH in comparison to CODH purified from *O. carboxidovorans* might result from a low level of MCD cofactor saturation, due to the unproductive expression of the accessory proteins required for MCD assembly and insertion in inclusion bodies. The saturation of the protein with the MCD cofactor conclusively needs to be optimized in future studies, by optimizing the expression of the proteins CoxDEF and CoxI. Nevertheless, this work provides the first heterologous expression system for an aerobic, bi-nuclear CO dehydrogenase in *E. coli* in an active form. A recent report by Choi et al.⁵¹ demonstrated the heterologous expression of the aerobic CODH from *Pantoea* species YR343 in *E. coli*. While the authors report on the characterization of an active enzyme that shows CO oxidation activity with different electron acceptors, no details on the saturation of the protein with cofactors are given. Since only the structural *coxMSL* proteins were expressed in *E. coli*, it remains elusive how a protein with a correctly assembled [MoO₂S-Cu] cluster was obtained. For example, the reconstitution of the copper-sulfur cluster was not required for the purified protein (instead the protein was reconstituted with FAD). Due to the lack of a quantification of the MCD cofactor, we are unable to compare our activities of the *O. carboxidovorans* CODH to the recombinantly obtained *Pantoea* CODH and suggest that the activity data reported by Choi et al.⁵¹ should be taken with care. Further, amino acid sequence analysis revealed that the protein is lacking the conserved "VAYRCSFR" loop present in Mo/Cu CODH enzymes,¹¹ which includes the cysteine corresponding to Cys388 in *O. carboxidovorans* CODH. Thus, it is likely that the *Pantoea* enzyme is not a Mo/Cu-containing CODH.

EPR spectroscopy has been employed as an important tool with respect to characterizing the mechanistic mode in the biotransformation of CO to CO₂ in Mo,Cu-CODHs. The electronically coupled Mo and Cu sites as Mo(V)-Cu(I) provide a diagnostic tool to assess how active site changes affect the electron centered at the MCD site. In our work herein, we show that heterologous expression of *O. carboxidovorans* CODH in *E. coli*, upon *in vitro* reconstitution with Cu(I) and sulfide under reducing conditions, resulted in a partially loaded enzyme, yielding similar EPR spectral properties to previous reports.^{39, 46} In almost all cases, the dithionite-reduced state was principally detected, even in the as-obtained state following reconstitution. This can be expected, since the reconstitution employed reducing conditions using dithionite as a reductant. Similarly, minor differences in the dithionite-reduced spectrum relative to previous reports may be due to overlapping H₂-reduced enzyme, since samples were prepared anaerobically in a H₂-containing Coy chamber.

It should be noted that the spin quantity of Mo(V)-associated signal is minor relative to the excess Cu(II) detected, particularly in the as-obtained state. The large quantity Cu(II)-derived spin in the as-obtained enzyme likely amounts to the amount of protein that lacks a loaded MCD cofactor, by which vacancy of the MCD cofactor likely results in oxidation of the delivered Cu(I) upon reconstitution to Cu(II) and that upon treatment of dithionite is cycled back to Cu(I). However, overall the heterologously expressed CODH in its dithionite-reduced state shows a similar coordination environment to that reported for natively expressed CODH, validating the employed reconstitution method and showing that the MCD-[MoO₂S-Cu] cofactor in the recombinant enzyme has identical features to the wild-type enzyme from *O. carboxidovorans*.

The successful establishment of a heterologous expression system in *E. coli* enabled us to perform site-directed mutagenesis of conserved amino acid residues at the active site. In particular we focused on the residues Glu763, Phe390 and Cys388. The exchange of Phe390 to a valine or proline in the active-site loop VAYRCSF³⁹⁰R resulted in the inability of the enzyme to oxidize CO or H₂. However, the loading of the enzyme with the MCD cofactor was also influenced by these amino acid exchanges. The X-ray structure of CODH showed that the inner side of the substrate access channel of CODH is flanked by hydrophobic residues^{8, 22} with Phe390 being located at the inner end of the channel in close proximity to active-site molybdenum and copper (7.4 and 5.9 Å, respectively). Phe390 was proposed to contribute to the dynamic flexibility of the enzyme, but also to sterically block the access of the substrates to the binuclear center.²⁷ Exchange of Phe390 to a valine replaces the aromatic phenylalanine by a short, non-aromatic and hydrophobic residue, which results in a disruption of the aromatic π -stacking between Phe390 and Phe355 and might thereby disturb the access of CO to the active site. Rokhsana et al.²⁸ reported by a theoretical approach on the interaction of Phe390 to be involved in the positioning of a water molecule to the Cu(I) center. The position of Phe390 was proposed to influence the nature of the Cu-OH₂ interaction and thereby to affect substrate binding and product release.²⁸ The exchange of phenylalanine by a valine conclusively might influence substrate binding and/or product release by resulting in a different active-site structure. Similar structural influences can be proposed for the F390P variant. Here the exceptional conformational rigidity of proline might also have an effect on the overall fold of the active-site loop. In contrast, the F390Y variant showed a residual activity for CO and H₂ oxidation, while the negative effect on CO oxidation was stronger than H₂ oxidation. Tyrosine is structurally related to phenylalanine with

the OH group in the para-position of the aromatic residue being the only difference. Thus, the F390Y variant allows the CO molecules to access the active site. Assuming the same orientation of the Tyr390 and the Phe390 residue in the active site, the additional OH group of tyrosine might interfere with Tyr568 that is located in close proximity (3.8 Å) on the G⁵⁶⁴LGTY⁵⁶⁸G⁵⁶⁹SRS loop. Consequently, this interference might displace Gly569 from its position in the active site. Gly569 is in close proximity (2.6 Å) to the equatorial oxo ligand of the molybdenum atom and might be involved in the stabilization of the oxo ligand.²⁸ Displacement of Gly569 from its position might further disturb this stabilizing effect and further influence the CO and H₂ oxidizing activities.

Cysteine in position 388 is part of the unique active-site loop (VAYRC³⁸⁸SF³⁹⁰R) and together with the μ -sulfido ligand, Cys388 ligates the Cu atom in the active-site of CODH.⁸ Deletion of Cys388 resulted in an inactive enzyme with an additional low saturation of the MCD cofactor. The deletion of Cys388 might also result in a shift of the active-site loop, thereby displacing the position of important residues for catalysis. However, the copper saturation of this variant was very high and might imply an unspecific copper accumulation of the enzyme, that might result in a not correctly assembled [MoO₃-S-Cu] cluster. The inactivity of the variant shows the importance of Cys388 for both CO and H₂ oxidation. Since we deleted the cysteine residue, we were unable to dissect the different role of the cysteine for CO and H₂ oxidation as predicted by Breglia et al.⁵² Here, the authors speculated that upon protonation of the cysteine, H₂ binding to copper is favored. In future studies, we plan to dissect the role of the cysteine for both substrate oxidation reactions in more detail.

Further, Glu763 is in close proximity (3 Å) to the equatorial hydroxo ligand of the Mo atom.⁸ During conversion of CO to CO₂, Glu763 was proposed recently by a

computational study to act as a base catalyst in deprotonation of a Mo-OH group further leading to a MoO₂ core and a protonated glutamate.²⁷ The Glu763 variant revealed to be completely inactive, while the MCD cofactor saturation was comparable to the WT enzyme. The essential role of this glutamate residue for CODH is consistent with the role of this highly conserved glutamate for other members of the XO family. So far, for all family member enzymes this glutamate residue was proven to be essential.

The data obtained in this work for the role of the amino acids Glu763, Phe390 and Cys388 for CO oxidation are summarized in Figure 11 and are consistent with the recent data by Rokhsana et al.²⁸, Breglia et al.⁵², the proposed mechanism by Stein and Kirk²⁴ and the mechanism suggested in Figure 5D of Hille et al.²⁷. After this model Glu763 might abstract a proton from water and produces the OH⁻ group, that then attacks the molybdenum-copper coordinated CO-intermediate at the active site (Figure 11A). However, the model initially proposed by Siegbahn and Shestakov (2005)²⁹ also can be applied with the essential role of Glu763 observed in this study (Figure 11B). In their proposed mechanism, Glu763 was suggested to have a key role at the very beginning of a proton transfer pathway essential for catalysis. Glu763 might abstract a proton from the Mo-OH group, as proposed for other enzymes of the xanthine oxidase family. After binding of CO to the Cu^I, a nucleophilic attack by the Mo-O⁻ group to the activated CO results in an initial intermediate as predicted before.

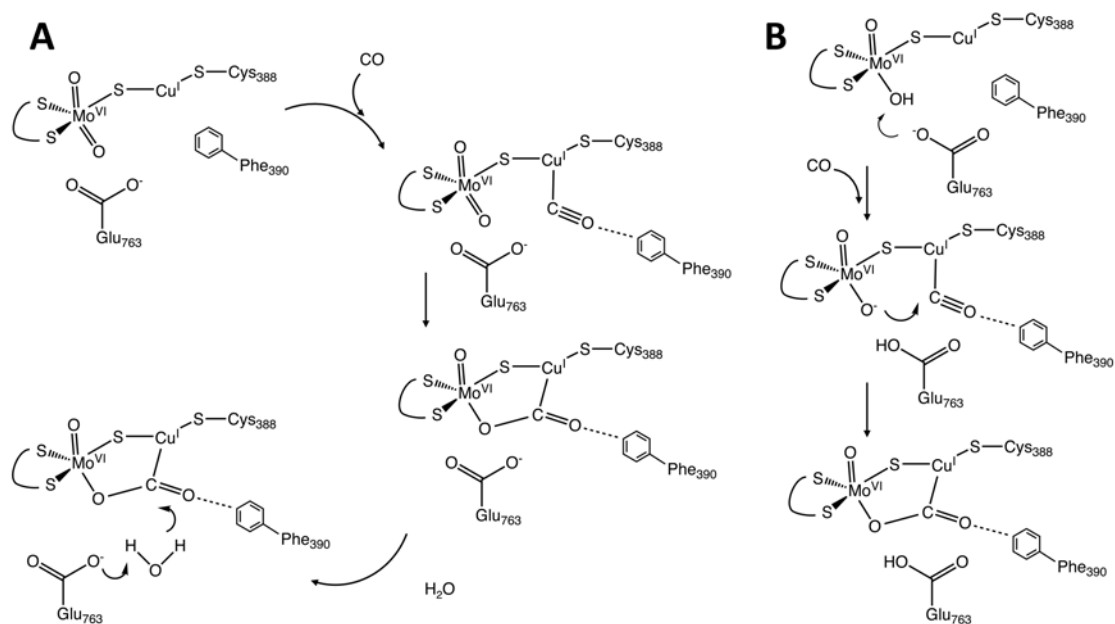


Figure 11: **Role of active-site amino acid residues for CO oxidation in CODH.** *A*, The CO-bound intermediate is shown in the active site after the mechanism described by Stein and Kirk.²⁴ A role of Glu763 is predicted in abstracting a proton from water that then acts as an OH⁻ intermediate. *B*, In the model proposed by Siegbahn and Shestakov (2005)²⁹ Glu763 was suggested to have a key role at the very beginning of the reaction. After this mechanism, Glu763 might abstract the proton from the Mo-OH group. After binding of CO to the Cu^I, a nucleophilic attack by the Mo-O⁻ group to the activated CO results in an initial intermediate. In both mechanisms, Phe390 might be involved in binding and positioning the substrate at the active-site.

Phe390 thereby is likely involved in binding and positioning of the substrate in the active-site. Alternatively, Glu763 might also be involved in modulating the redox potential of the active site, or also might have a structural role in assisting the assembly of the [MoO₂S-Cu] active site. More details of the exact roles of the amino acid residues have to be investigated in future studies by a combination of X-ray crystallography and various spectroscopic methods.

AUTHOR INFORMATION

Corresponding Author

*To whom correspondence should be addressed: Silke Leimkühler, Institute of Biochemistry and Biology, Department of Molecular Enzymology, University of Potsdam, Karl-Liebknecht-Str. 24-25, 14476 Potsdam, Germany, Telephone: +49-331-977-5603; Fax: +49-331 977-5128; E-mail: sleim@uni-potsdam.de

FUNDING

This work was supported by the cluster of excellence 314 “Unicat” (to C.T. and S.L.), funded by the DFG.

NOTES:

The authors declare they have no conflicts of interest with the contents of this article.

ACKNOWLEDGEMENTS

We thank Angelika Lehmann (Potsdam) for protein purification and technical assistance. We further thank Russ Hille (UC Riverside), Jarett Wilcoxon and the Alexander von Humboldt foundation for initiating this project. Russ Hille provided the initial idea to express *O. carboxidovorans* CODH in *E. coli* and the megaplasmid pHCG3 for cloning experiments. Jarett Wilcoxon started the initial cloning experiments. This part of the project was funded by an Alexander von Humboldt research prize awarded to Russ Hille that allowed him a research stay at the University of Potsdam.

SUPPORTING INFORMATION AVAILABLE

Supplementary Table S1, S2 and Figure S1.

Table S1: Quantification of metals, cofactors and specific activities of CODH expressed from different gene combinations in *E. coli*.

Table S2: Quantification of metals, cofactors and specific activities of CODH active-site variants.

Figure S1: 17% SDS-PAGE of CODH proteins purified after expression in *E. coli*.

REFERENCES

- [1] Meyer, O., and Schlegel, H. G. (1983) Biology of aerobic carbon monoxide-oxidizing bacteria, *Annu Rev Microbiol* 37, 277-310.
- [2] Meyer, O., and Schlegel, H. G. (1978) Reisolation of the carbon monoxide utilizing hydrogen bacterium *Pseudomonas carboxydovorans* (Kistner) comb. nov, *Arch Microbiol* 118, 35-43.
- [3] Wilcoxon, J., Zhang, B., and Hille, R. (2011) Reaction of the molybdenum- and copper-containing carbon monoxide dehydrogenase from *Oligotropha carboxydovorans* with quinones, *Biochemistry* 50, 1910-1916.
- [4] Meyer, O., Jacobitz, S., and Krüger, B. (1986) Biochemistry and physiology of aerobic carbon monoxide-utilizing bacteria, *FEMS Microbiol. Rev.* 39, 161-179.
- [5] Moxley, J., and Smith, K. (1998) Factors affecting utilisation of atmospheric CO by soils, *Soil Biology and Biochemistry* 30, 65-79.
- [6] Mörsdorf, G., Frunzke, K., Gadkari, D., and Meyer, O. (1992) Microbial growth on carbon monoxide, *Biodegradation* 3, 61-82.
- [7] Hille, R. (1996) The mononuclear molybdenum enzymes, *Chemical Rev* 96, 2757-2816.
- [8] Dobbek, H., Gremer, L., Kiefersauer, R., Huber, R., and Meyer, O. (2002) Catalysis at a dinuclear [CuSMo(=O)OH] cluster in a CO dehydrogenase resolved at 1.1-Å resolution, *Proc Natl Acad Sci U S A* 99, 15971-15976.
- [9] Gnida, M., Ferner, R., Gremer, L., Meyer, O., and Meyer-Klaucke, W. (2003) A novel binuclear [CuSMo] cluster at the active site of carbon monoxide dehydrogenase: characterization by X-ray absorption spectroscopy, *Biochemistry* 42, 222-230.

- [10] Kraut, M., Hugendieck, I., Herwig, S., and Meyer, O. (1989) Homology and distribution of CO dehydrogenase structural genes in carboxydophilic bacteria, *Arch Microbiol* 152, 335-341.
- [11] Santiago, B., Schubel, U., Egelseer, C., and Meyer, O. (1999) Sequence analysis, characterization and CO-specific transcription of the *cox* gene cluster on the megaplasmid pHCG3 of *Oligotropha carboxidovorans*, *Gene* 236, 115-124.
- [12] Pelzmann, A., Ferner, M., Gnida, M., Meyer-Klaucke, W., Maisel, T., and Meyer, O. (2009) The CoxD protein of *Oligotropha carboxidovorans* is a predicted AAA+ ATPase chaperone involved in the biogenesis of the CO dehydrogenase [CuSMoO₂] cluster, *J Biol Chem* 284, 9578-9586.
- [13] Maisel, T., Joseph, S., Mielke, T., Burger, J., Schwarzingler, S., and Meyer, O. (2012) The CoxD protein, a novel AAA+ ATPase involved in metal cluster assembly: hydrolysis of nucleotide-triphosphates and oligomerization, *PLoS One* 7, e47424.
- [14] Pelzmann, A. M., Mickoleit, F., and Meyer, O. (2014) Insights into the posttranslational assembly of the Mo-, S- and Cu-containing cluster in the active site of CO dehydrogenase of *Oligotropha carboxidovorans*, *J Biol Inorg Chem* 19, 1399-1414.
- [15] Neumann, M., Schulte, M., Jünemann, N., Stöcklein, W., and Leimkühler, S. (2006) *Rhodobacter capsulatus* XdhC is involved in molybdenum cofactor binding and insertion into xanthine dehydrogenase, *J Biol Chem* 281, 15701-15708.
- [16] Neumann, M., Stöcklein, W., and Leimkühler, S. (2007) Transfer of the Molybdenum Cofactor Synthesized by *Rhodobacter capsulatus* MoeA to XdhC and MobA, *J Biol Chem* 282, 28493-28500.

- [17] Neumann, M., Stöcklein, W., Walburger, A., Magalon, A., and Leimkühler, S. (2007) Identification of a *Rhodobacter capsulatus* L-cysteine desulfurase that sulfurates the molybdenum cofactor when bound to XdhC and before its insertion into xanthine dehydrogenase, *Biochemistry* 46, 9586-9595.
- [18] Lamont, C. M., Kelly, C. L., Pinske, C., Buchanan, G., Palmer, T., and Sargent, F. (2017) Expanding the substrates for a bacterial hydrogenlyase reaction, *Microbiology*.
- [19] Fuhrmann, S., Ferner, M., Jeffke, T., Henne, A., Gottschalk, G., and Meyer, O. (2003) Complete nucleotide sequence of the circular megaplasmid pHCG3 of *Oligotropha carboxidovorans*: function in the chemolithoautotrophic utilization of CO, H₂ and CO₂, *Gene* 322, 67-75.
- [20] Neumann, M., and Leimkühler, S. (2011) The role of system-specific molecular chaperones in the maturation of molybdoenzymes in bacteria, *Biochem Res Int* 2011, 850924.
- [21] Wilcoxon, J., and Hille, R. (2013) The hydrogenase activity of the molybdenum/copper-containing carbon monoxide dehydrogenase of *Oligotropha carboxidovorans*, *J Biol Chem* 288, 36052-36060.
- [22] Dobbek, H., Gremer, L., Meyer, O., and Huber, R. (1999) Crystal structure and mechanism of CO dehydrogenase, a molybdo iron-sulfur flavoprotein containing S-selenylcysteine, *Proc. Natl. Acad. Sci. U. S. A.* 96, 8884-8889.
- [23] Shanmugam, M., Wilcoxon, J., Habel-Rodriguez, D., Cutsail Iii, G. E., Kirk, M. L., Hoffman, B. M., and Hille, R. (2013) (13)C and (63,65)Cu ENDOR studies of CO Dehydrogenase from *Oligotropha carboxidovorans*. Experimental Evidence in Support of a Copper-Carbonyl Intermediate, *J Am Chem Soc* 135, 17775-17782.

- [24] Stein, B. W., and Kirk, M. L. (2014) Orbital contributions to CO oxidation in Mo-Cu carbon monoxide dehydrogenase, *Chem Commun (Camb)* 50, 1104-1106.
- [25] Breglia, R., Bruschi, M., Cosentino, U., De Gioia, L., Greco, C., Miyake, T., and Moro, G. (2016) A theoretical study on the reactivity of the Mo/Cu-containing carbon monoxide dehydrogenase with dihydrogen, *Protein Engineering, Design and Selection* 30, 169-174.
- [26] Meyer, O., Gremer, L., Ferner, R., Ferner, M., Dobbek, H., Gnida, M., Meyer-Klaucke, W., and Huber, R. (2000) The role of Se, Mo and Fe in the structure and function of carbon monoxide dehydrogenase, *Biol Chem* 381, 865-876.
- [27] Hille, R., Dingwall, S., and Wilcoxon, J. (2015) The aerobic CO dehydrogenase from *Oligotropha carboxidovorans*, *J Biol Inorg Chem* 20, 243-251.
- [28] Rokhsana, D., Large, T. A., Dienst, M. C., Retegan, M., and Neese, F. (2016) A realistic in silico model for structure/function studies of molybdenum-copper CO dehydrogenase, *J Biol Inorg Chem* 21, 491-499.
- [29] Siegbahn, P. E., and Shestakov, A. F. (2005) Quantum chemical modeling of CO oxidation by the active site of molybdenum CO dehydrogenase, *Journal of computational chemistry* 26, 888-898.
- [30] Hille, R., Hall, J., and Basu, P. (2014) The mononuclear molybdenum enzymes, *Chemical reviews* 114, 3963-4038.
- [31] Neumann, M., Mittelstädt, G., Iobbi-Nivol, C., Saggiu, M., Lenzian, F., Hildebrandt, P., and Leimkühler, S. (2009) A periplasmic aldehyde oxidoreductase represents the first molybdopterin cytosine dinucleotide cofactor containing molybdo-flavoenzyme from *Escherichia coli*, *The FEBS journal* 276, 2762-2774.

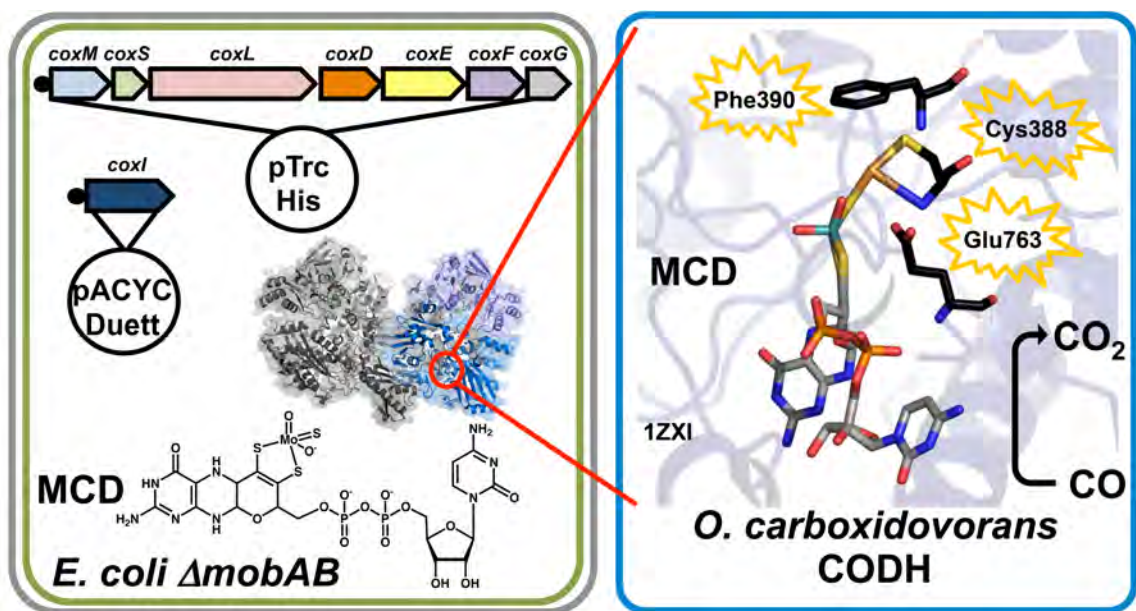
- [32] Neumann, M., Mittelstädt, G., Seduk, F., Iobbi-Nivol, C., and Leimkühler, S. (2009) MocA is a specific cytidylyltransferase involved in molybdopterin cytosine dinucleotide biosynthesis in *Escherichia coli*, *J Biol Chem* 284, 21891-21898.
- [33] Temple, C. A., and Rajagopalan, K. V. (2000) Optimization of Expression of Human Sulfite Oxidase and its Molybdenum Domain, *Arch. Biochem. Biophys.* 383, 281-287.
- [34] Palmer, T., Santini, C.-L., Iobbi-Nivol, C., Eaves, D. J., Boxer, D. H., and Giordano, G. (1996) Involvement of the *narJ* and *mob* gene products in the biosynthesis of the molybdoenzyme nitrate reductase in *Escherichia coli*, *Mol Microbiol* 20, 875-884.
- [35] Stewart, V., and MacGregor, C. H. (1982) Nitrate reductase in *Escherichia coli* K-12: involvement of *chlC*, *chlE*, and *chlG* loci, *J. Bacteriol.* 151, 788-799.
- [36] Johnson, J. L., Rajagopalan, K. V., and Meyer, O. (1990) Isolation and characterization of a second molybdopterin dinucleotide: molybdopterin cytosine dinucleotide, *Arch. Biochem. Biophys.* 283, 542-545.
- [37] Massey, V., and Edmondson, D. (1970) On the mechanism of inactivation of xanthine oxidase by cyanide, *J. Biol. Chem.* 245, 6595-6598.
- [38] Meyer, O., and Schlegel, H.-G. (1980) Carbon monoxide: methylene blue oxidoreductase from *Pseudomonas carboxydovorans*, *J Bacteriol* 141, 74-80.
- [39] Resch, M., Dobbek, H., and Meyer, O. (2005) Structural and functional reconstruction in situ of the [CuSMoO₂] active site of carbon monoxide dehydrogenase from the carbon monoxide oxidizing eubacterium *Oligotropha carboxidovorans*, *J Biol Inorg Chem* 10, 518-528.

- [40] Hartmann, T., and Leimkühler, S. (2013) The oxygen-tolerant and NAD-dependent formate dehydrogenase from *Rhodobacter capsulatus* is able to catalyze the reduction of CO to formate, *The FEBS journal* 280, 6083-6096.
- [41] Niks, D., Duvvuru, J., Escalona, M., and Hille, R. (2016) Spectroscopic and Kinetic Properties of the Molybdenum-containing, NAD⁺-dependent Formate Dehydrogenase from *Ralstonia eutropha*, *J Biol Chem* 291, 1162-1174.
- [42] Wilcoxon, J., and Hille, R. (2013) The Hydrogenase Activity of the Mo/Cu Containing Carbon Monoxide Dehydrogenase of *Oligotropha carboxidovorans*, *J Biol Chem*.
- [43] Leimkühler, S., Hodson, R., George, G. N., and Rajagopalan, K. V. (2003) Recombinant *Rhodobacter capsulatus* xanthine dehydrogenase, a useful model system for the characterization of protein variants leading to xanthinuria I in humans, *J Biol Chem* 278, 20802-20811.
- [44] Hartmann, T., Terao, M., Garattini, E., Teutloff, C., Alfaro, J. F., Jones, J. P., and Leimkühler, S. (2012) The impact of single nucleotide polymorphisms on human aldehyde oxidase, *Drug Metab Dispos* 40, 856-864.
- [45] Leimkühler, S., Hodson, R., George, G. N., and Rajagopalan, K. V. (2003) Recombinant *Rhodobacter capsulatus* xanthine dehydrogenase, a useful model system for the characterization of protein variants leading to xanthinuria I in humans, *J Biol Chem* 278, 20802-20811.
- [46] Zhang, B., Hemann, C. F., and Hille, R. (2010) Kinetic and spectroscopic studies of the molybdenum-copper CO dehydrogenase from *Oligotropha carboxidovorans*, *J Biol Chem* 285, 12571-12578.
- [47] Gremer, L., Kellner, S., Dobbek, H., Huber, R., and Meyer, O. (2000) Binding of flavin adenine dinucleotide to molybdenum-containing carbon monoxide

- dehydrogenase from *Oligotropha carboxidovorans*. Structural and functional analysis of a carbon monoxide dehydrogenase species in which the native flavoprotein has been replaced by its recombinant counterpart produced in *Escherichia coli*, *J Biol Chem* 275, 1864-1872.
- [48] Heinrich, D., Raberg, M., and Steinbuchel, A. (2017) Studies on the aerobic utilization of synthesis gas (syngas) by wild type and recombinant strains of *Ralstonia eutropha* H16, *Microb Biotechnol*.
- [49] Hänzelmann, P., Dobbek, H., Gremer, L., Huber, R., and Meyer, O. (2000) The effect of intracellular molybdenum in *Hydrogenophaga pseudoflava* on the crystallographic structure of the seleno-molybdo-iron-sulfur flavoenzyme carbon monoxide dehydrogenase, *J Mol Biol* 301, 1221-1235.
- [50] Hänzelmann, P., and Meyer, O. (1998) Effect of molybdate and tungstate on the biosynthesis of CO dehydrogenase and the molybdopterin cytosine-dinucleotide-type of molybdenum cofactor in *Hydrogenophaga pseudoflava*, *Eur. J. Biochem.* 255, 755-765.
- [51] Choi, E. S., Min, K., Kim, G. J., Kwon, I., and Kim, Y. H. (2017) Expression and characterization of *Pantoea* CO dehydrogenase to utilize CO-containing industrial waste gas for expanding the versatility of CO dehydrogenase, *Sci Rep* 7, 44323.
- [52] Breglia, R., Bruschi, M., Cosentino, U., De Gioia, L., Greco, C., Miyake, T., and Moro, G. (2017) A theoretical study on the reactivity of the Mo/Cu-containing carbon monoxide dehydrogenase with dihydrogen, *Protein Eng Des Sel* 30, 167-172.

For table of contents use only

*Functional studies on Oligotropha
carboxidovorans molybdenum-copper CO
dehydrogenase produced in Escherichia coli*



Supporting Information:

*Functional studies on Oligotropha carboxidovorans
molybdenum-copper CO dehydrogenase produced in
Escherichia coli*

Paul Kaufmann¹, Benjamin R. Duffus¹, Christian Teutloff² and Silke Leimkühler^{1}*

From the ¹Institute of Biochemistry and Biology, Department of Molecular Enzymology,
University of Potsdam, 14476 Potsdam, Germany.

²Institute for Experimental Physics, Free University of Berlin, Arnimallee 14, 14195 Berlin,
Germany.

TABLE OF CONTENTS

Supplementary Table

Table S1: **Quantification of metals and cofactors of CODH expressed from different gene combinations in *E. coli*.**

Table S2: **Quantification of metals, cofactors and specific activities of CODH active-site variants.**

Supplementary Figures

Figure S1: **17% SDS-PAGE of CODH proteins purified after expression in *E. coli*.**

Table S1: Quantification of metals and cofactors of CODH expressed from different gene combinations in *E. coli*.

<i>E. coli</i> strain	Expressed genes	Yield in mg/L culture ^a	Saturation in %					
			Mo ^{a,b}	Fe ^{a,b}	Cu ^{a,b}	S ^{a,b}	FAD ^{a,c}	CMP ^{a,c}
RK5200 (DE3)	<i>coxMSLDEFG</i> + <i>coxHI</i>	5.9	11 ±4	106 ±10	59 ±7	40 ±0.5	89 ±7	15 ±0.8
TP1000 (DE3)	<i>coxMSLDEFG</i>	7.1	22 ±4	91 ±12	43 ±5	28 ±1.3	80 ±1	12 ±1
TP1000 (DE3)	<i>coxMSLDEFG</i> + <i>coxHI</i>	5.9	41 ±7	104 ±8	48 ±7	65 ±12	79 ±7	54 ±10
TP1000 (DE3)	<i>coxMSLDEFG</i> + <i>coxH</i>	5.8	23 ±6	88 ±12	44 ±9	52 ±2	91 ±10	40 ±2
TP1000 (DE3)	<i>coxMSLDEFG</i> + <i>coxI</i>	5.3	26 ±7	104 ±4	58 ±3	68 ±4	96 ±6	58 ±3

^aMolybdenum ($\mu\text{M Mo}/\mu\text{M CODH}$), iron ($\mu\text{M } 2\text{x}[2\text{Fe}_2\text{S}_2]/\mu\text{M CODH}$) and copper ($\mu\text{M Cu}/\mu\text{M CODH}$) contents were determined by ICP-OES (see Materials and Methods) and related to a fully saturated enzyme. The concentration of the terminal sulfur ligand of Moco ($\mu\text{M SCN}/\mu\text{M CODH}$) was determined spectrophotometrically as an iron-thiocyanate complex at 420 nm as described in Materials and Methods. Potassium thiocyanate was used as a standard curve. FAD was quantified spectroscopically after TCA precipitation of the protein as described in Experimental procedures. The CMP content ($\mu\text{M CMP}/\mu\text{M CODH}$) was analyzed after release of CMP from MCD by heat treatment under acidic conditions, as described in Materials and Methods.

^bDetermined before *in vitro* reconstitution of the purified enzyme with copper and sulfide.

^cDetermined after *in vitro* reconstitution of the purified enzyme with copper and sulfide.

Table S2: Quantification of metals, cofactors and specific activities of CODH active-site variants.

CODH variant	Yield in mg/L culture ^a	Saturation in %						Specific activity in mU/mg ^a	
		Mo ^{a,b}	Fe ^{a,b}	Cu ^{a,b}	S ^{a,b}	FAD ^{a,c}	CMP ^{a,c}	CO	H ₂
E763Q	6.1	63 ±9	110 ±10	69 ±3	51 ±10	86 ±1	58 ±8	n.d.	n.d.
F390P	2.3	14 ±4	99 ±4	64 ±5	46 ±4	87 ±3	26 ±8	n.d.	n.d.
F390V	2.5	8 ±1	97 ±6	125 ±12	48 ±8	76 ±1	38 ±12	n.d.	n.d.
F390Y	6.7	17 ±0.1	97 ±5	67 ±5	59 ±7	76 ±1	46 ±9	40± 3	15±1
ΔC388	4.1	28 ±17	97 ±2	99 ±13	33 ±7	96 ±16	43 ±8	n.d.	n.d.

^aSpecific enzyme activities (U/mg) are defined as the oxidation of 1 μmol substrate/mg enzyme. Molybdenum (μM molybdenum/μM CODH), iron (μM 2x[2Fe2S]/μM CODH) and copper (μM copper/μM CODH) contents were determined by ICP-OES (see Materials and Methods) and related to a fully saturated enzyme. The concentration of the terminal sulfur ligand of Moco (μM SCN)/μM CODH) was determined spectrophotometrically as an iron-thiocyanate complex at 420 nm as described in Materials and Methods. Potassium thiocyanate was used as a standard curve. FAD was quantified spectroscopically after TCA precipitation of the protein as described in Experimental procedures. The CMP content (μM CMP/μM CODH) was analyzed after release of CMP from MCD by heat treatment under acidic conditions, as described in Materials and Methods.

^bDetermined before *in vitro* reconstitution of the purified enzyme with copper and sulfide.

^cDetermined after *in vitro* reconstitution of the purified enzyme with copper and sulfide.

n.d.: no activity detectable

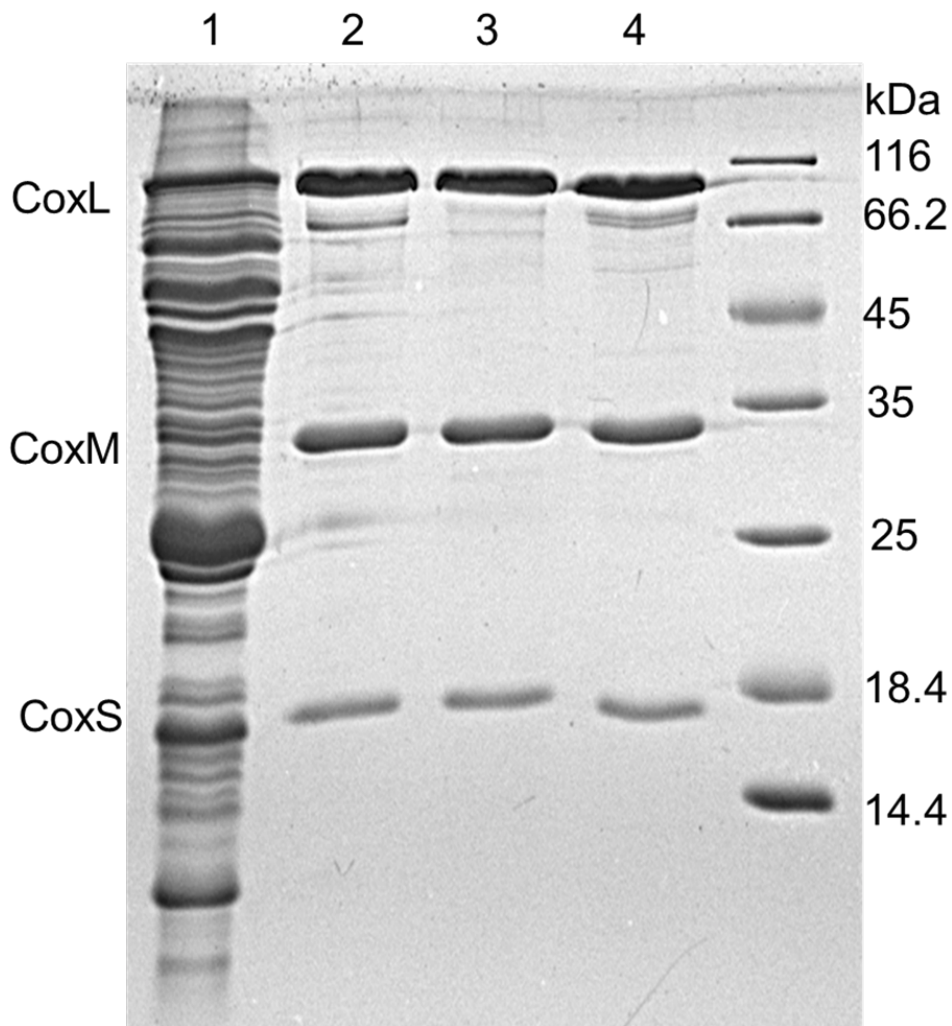


Figure S1: 17% SDS-PAGE of CODH proteins purified after expression in *E. coli*.

Lane 1: Ni-NTA purification after expression of *coxMSL* from pPK1 at 16 °C. Lane 2: Ni-NTA purification after expression of *coxMSLDEFG* from pPK2 at 16 °C. Lane 3: Ni-NTA purification after coexpression of *coxMSLDEFG* with *coxH* and *coxI* from pPK2 and pPK3 at 16 °C. Lane 4: Ni-NTA purification after coexpression of *coxMSLDEFG* with *coxH* and *coxI* from pPK2 and pPK3 at 30 °C. Proteins were stained with Coomassie brilliant blue.